ENGINEERING TRANSACTIONS

ROZPRAWY INŻYNIERSKIE - TRAITE d'INGENIERIE

SUBSCRIPTIONS

Due to the signed agreement between the director of the Institute of Fundamental Technological Research of the Polish Academy of Sciences in Warsaw, Professor ANDRZEJ NOWICKI, and the director of the National Engineering School of Metz – ENIM – Professor PIERRE PADILLA, about the joint publishing since 2011 of the Quarterly Journal *ENGINEERING TRANSACTIONS* (*ROZPRAWY INŻYNIERSKIE – TRAITE d'INGENIERIE*), our Quarterly founded in 1952 by WITOLD NOWACKI, WACŁAW OLSZAK and WITOLD WIERZBICKI has been set on a new path of its development. We consider this to be a milestone strengthening of the international position of the journal and aiming at the publishing market of the European Research Area. This goal will be accomplished by the newly formed Editorial Committee and the International Committee. This joint undertaking is in accordance with the thought of MARIA SKŁODOWSKA–CURIE: *After all, science is essentially international, and it is only through lack of the historical sense that national qualities have been attributed to it.* (Memorandum of the International Committee on Intellectual Co-operation: Sub-committee of Experts for the . . . Aims of the League of Nations. (Recommendations. Preamble): Issues 9–13, 1926).

It seems to be a good sign that we start our editorial French–Polish cooperation in the year 2011, which has been declared by France and Poland the Year of MARIA SKŁODOWSKA–CURIE (1867–1934) – the most famous woman scientist and twice the winner of the Nobel Prize, born in Warsaw. She was the first female professor in the history of the Sorbonne, and the French government decorated her with the Legion of Honour. She is the only woman and the only person not born in France, who has been buried in the Paris Panthéon. She received her first Nobel Prize in physics in 1903 (together with her husband Pierre Curie and Henri Becquerel), and the second one alone in 1911 (in chemistry). The life of Maria Skłodowska–Curie was closely connected with Warsaw and Paris. From her studies at the Sorbonne until the end of her life she lived in France, but she visited Warsaw very often and there are many places in this city, which are reminiscent of her.

Editorial Committee

DAMAGE REDUCTION OF EXPLOSIVELY DRIVEN SPALLATION BY MACHINING V-NOTCH ROWS ON THE SURFACES OF 304 STAINLESS STEEL PLATES

T. H i r o e [1)], K. F u j i w a r a [1)], H. H a t a [1)],
K. N a t a s a t o [2)], K. M i z o k a m i [2)]

[1)] **Department of Mechanical System Engineering, Kumamoto University**
Kumamoto, 860-8555, Japan
e-mail: hiroe@gpo.kumamoto-u.ac.jp

[2)] **Graduate School of Science and technology, Kumamoto University**
Japan

Plane detonation waves generated in the explosive PETN with use of wire-row explosion technique for initiation have been applied to study on spall behaviour for circular plates of 304 stainless steel, and the slanting surface effects on the damage phenomena for conic frustums and circular cones. In this paper, V-notch rows are produced on the free surface of the square plate specimens of the same material and plane shock waves are similarly transferred from the other surface. The cross-sectional observation of tested and recovered specimens shows that remarkable effects on the reduction of spall damages have been achieved in case of appropriate V-notch configurations. The effect seems to come obviously from weakened interaction of release waves due to the dispersion of directions for reflection waves, and a hydro-code. Autodyn 2D/3D has successfully reproduced the experimental results numerically, suggesting a notch parameter chart for spall damage evaluation.

1. Introduction

Spallation driven by direct explosive loadings [1] occurs due to tensile stresses generated by the interaction of expansion waves emerged due to the reflection of strong shock waves at the free surfaces of the structural components and other strong expansion waves coming from behind the detonation waves. Previously, the authors [2] had developed explosive loading devices producing planar detonation waves in powder pentaerythritoltetranitrate (PETN) with the use of exploding copper wire rows for initiation, showing some applications to spall tests for circular plane plates of various metallic materials, where the spalling phenomena were monitored by VISAR signals. In the following study [3, 4], spallation driven by direct explosive loads was similarly investigated for additional two types of specimens: conical frustums and circular cones of aluminum alloys and a stainless steel with variations of specimen configurations and explosive

heights, and the experimental results revealed that slanting side surfaces change the spall damage phenomena showing a possibility to reduce spall failure by applying such effects. Typical related test data are shown in Fig. 1. In this paper, V-notch rows are newly produced on the free surfaces of the stainless steel plate specimens and the explosive loading tests are performed investing appropriate V-notch configurations for spall damage reduction by means of numerical simulations.

a) circular plate

b) conical frustum
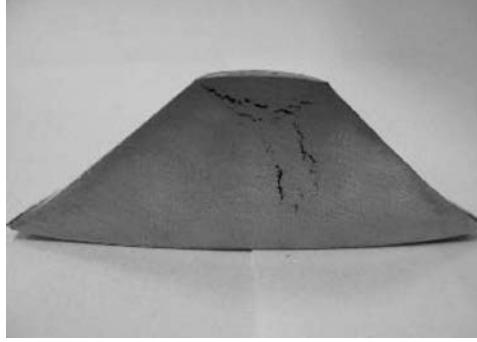
c) VISAR signal
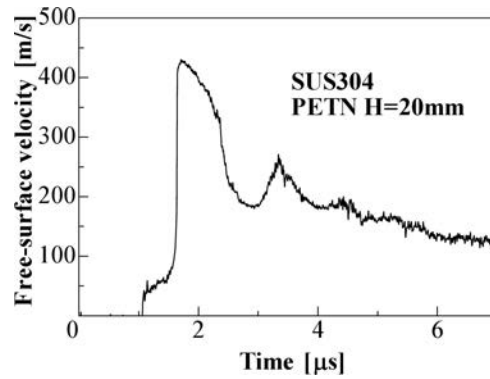
FIG. 1. Previous spall test data [2–4] of a stainless steel (SUS304) with PETN height H of 20 mm: cross-sectional photos of recovered: a) circular plate (ϕ: 50 mm, t: 20 mm), b) conical frustum (ϕ_1/ϕ_2: 12 mm/50 mm, sloping 43.5 deg.), and c) a typical VISAR signal.

2. EXPERIMENTAL AND NUMERICAL PROCEDURE

Experiments are performed using the explosion test facilities at the Shock Wave and Condensed Matter Research Center, Kumamoto University. Schematic experimental assembly for direct-explosive impact tests is shown, with the configuration parameters of tested specimens, in Fig. 2. Slab-like installed powder PETN (0.90–0.95 g/cc) is initiated by the simultaneous explosion of parallel
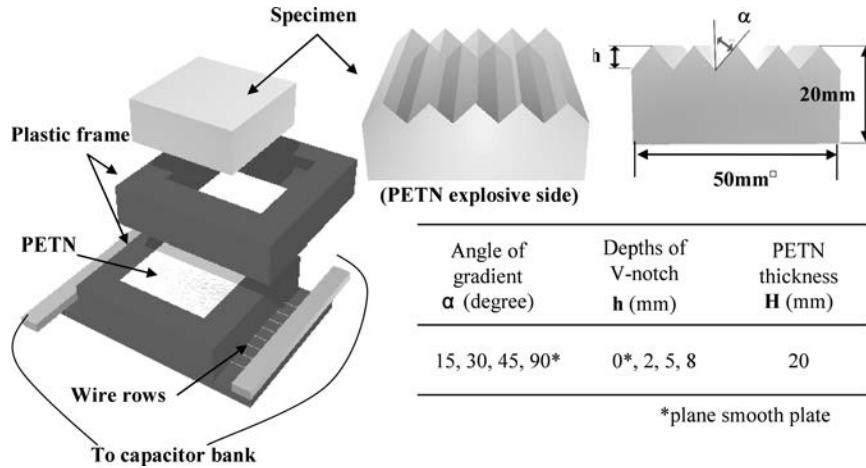
FIG. 2. Schematics of experimental assembly and the configuration parameters of tested specimens in this study.

copper wire rows (diameter: 175 μm, the ratio of PETN thickness H of wire interval B, H/B≥1.3–1.5 for planarity [2]), placed over the entire outer surface using an impulsive discharge current from a capacitor bank of 40 μF, 20 kV, producing a planar detonation front in the PETN layer immediately after the initial explosion and transferring a one-dimensional triangular pressure pulse directly to the specimen plate. The PETN is installed constantly in the shape of 50×50×20 mm and the wire intervals are 7–8 mm in the experiments. The specimens of 18Cr-8Ni stainless steel, JIS SUS304 are machined to the smooth quadratic plates of 50×50×20 mm from the rolled plate of thickness of 25 mm as a basic specimen and in this study, V-notch rows were newly produced parallel to the side lines by electro-discharge machining on the free surfaces of the specimens with notch variation of height or depth h of 2, 5, 8 mm and gradient angles α of 15, 30, 45 degrees respectively. Numerical simulations are performed for all the experiments and additional conditions using a hydro-code: Autodyn 2D/3D based on the finite difference method, and Euler coordinates, material data or 304 stainless steel [5], PETN and plastics built in the code, and two-dimensional analysis with mesh division of 0.2×0.2 mm, are basically employed here. Stress criterion of SUS304: $\sigma_{sp} = 3.5$ GPa previously obtained [2] shown in Fig. 1c for spall damage has been also adopted.

3. EXPERIMENTAL RESULTS

In all the explosion tests, experimental assembly shown in Fig. 2 was installed inside a cushion-filled chamber set in the pit and the tested specimens were successfully recovered without secondary damage. The recovered speci-

mens were separated halves by a fine-cutter machine perpendicularly to V-notch rows and the emerged cross-sectional surfaces were lapped. Spall damages of the specimens were observed in the cross-sections for all the cases. Figure 3 shows cross-sectional photos of tested specimens for all the notched specimens, and macroscopic observation indicates three types of damage phenomena in the cross-sections. In the first type, spall damages extended parallel to the plate surfaces or perpendicular to stress wave propagation. It is the ordinary spallation caused by the interaction of the expansion wave reflected at the free surfaces of the plate specimen and other expansion wave coming from behind the detonation. Here it is called "horizontal spall", as shown in the figure. In the second type called "vertical spall", spall damages extended along the central line of each ridge of the V-notch rows. This type of damages are obviously caused by the interaction of expansion waves reflected at a pair of slanting surfaces on every V-notch row, and then in this case, ordinary spallation does not appear because of reduction of the reflected expansion waves. Finally, in the third type called "no spall", only the case of $\alpha = 15°$, $h = 8$ mm, spall damage is remarkably reduced almost to zero under the macroscopic observation, where around 0.4 mm cracking is critical. Additionally, a mixed type of horizontal and vertical spall exists consequently what is seen in the case of $\alpha = 30°$, $h = 5$ mm.
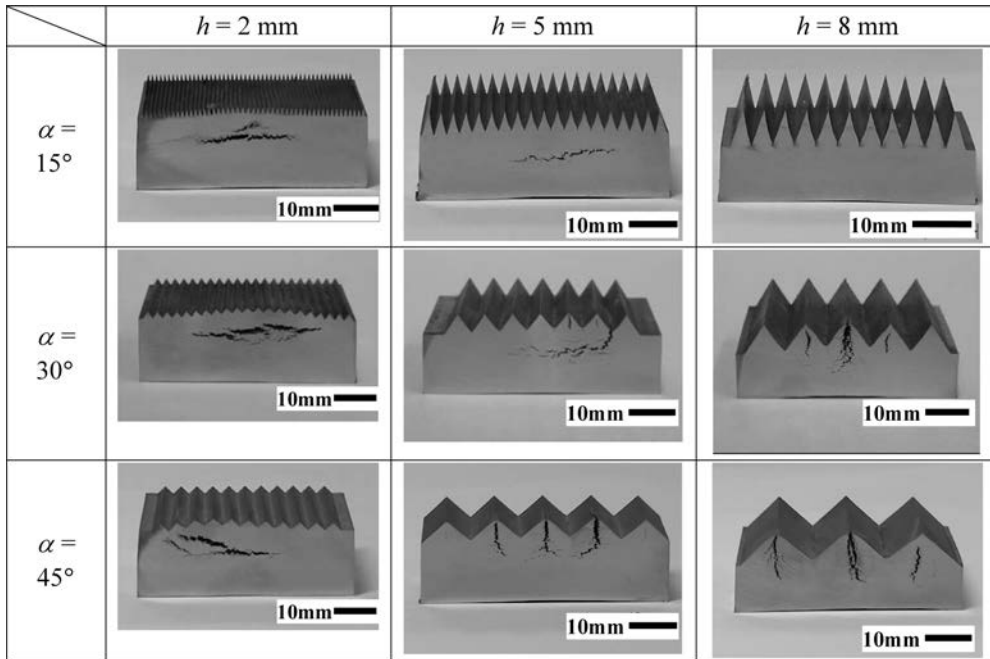
FIG. 3. Cross-sectional photos of tested, recovered and half-cut specimens for all the notched specimens.

4. Numerical results

In preliminary investigation, numerical overall spall damage phenomena in the cross-sections generated 3D analysis of Autodyn do not make essential difference from those by 2D analysis, and actually in this study, 2D numerical simulation successfully reproduced experimental cross-sectional spall damages for all the cases. Figure 4 shows typical three types of numerical damage distributions in the cross-sections based on stress criterion, where lowermost density elements are represented as voids. They correspond practically well to experimental results shown in Fig. 3 including no spall type, where separation of two meshes is defined as numerical minimum damage coinciding with experimental macroscopic observation. Next in order to verify the emerged damage phenomena on the stress criterion base, stresses in the specimens were examined for all the test cases. Figure 5 shows typical numerical time-histories of spatial distri-

Types	Horizontal spall	Vertical spall	No spall damage
Typical examples			
Parameter	$\alpha = 30°$, $h = 2$ mm	$\alpha = 45°$, $h = 8$ mm	$\alpha = 15°$, $h = 8$ mm

FIG. 4. Typical three types of numerical simulation results for the cross-sections of explosively loaded, notched specimens with use of Autodyn 2D. Solid lines show 10 mm.

a) $\alpha = 30°$, $h = 2$ mm   b) $\alpha = 45°$, $h = 8$ mm   c) $\alpha = 15°$, $h = 8$ mm
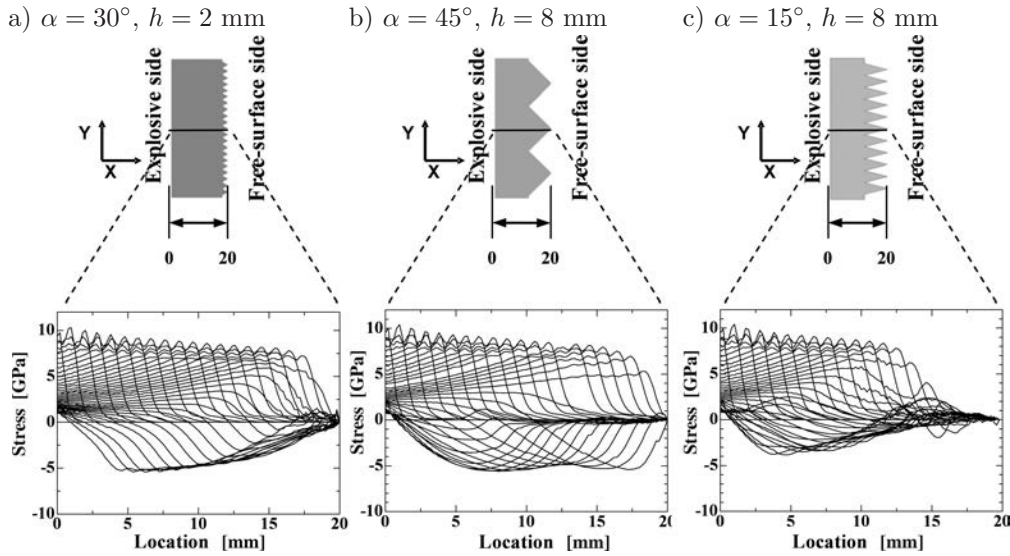
FIG. 5. Typical numerical time- histories of spatial distributions of stress $\sigma_x (\cong \sigma_y)$ in the specimens shown in Fig. 4.

butions of stress $\sigma_x (\cong \sigma_y)$, along the central line from the bottom of the plate to the peak of the V-notch ridge in the same specimens in Fig. 4, where x and y are the directions of thickness and width of the plate perpendicular to the notch rows, and plus stress denotes a compressive one, and failure criterion is not used here. It is seen that in cases (a) and (b), reflected tensile stresses soon go much over the stress criterion value σ_{sp} of 3.5 GPa, and in case (c) the stresses barely reach the value in a short period after some time period from the reflection at the restricted narrow area. The damages in the specimens with lowest notch height of 2 mm in the case (a) resemble that of plane smooth plate without slant surface effect, and it follows from small stress growth and interaction after reflection. Such stress distributions explain well all the spall phenomena in this study.

5. DISCUSSION

Experimental and numerical results suggest that there exists a notch parameter chart for spall damage evaluation. In the numerical simulation for building the chart, 2D analysis for the model including only one ridge of V-notch assuming wide plate with large number of notch rows, was adopted for simplicity as the damage evaluation model of central part in the specimen, which is confirmed appropriately as a practical use by preliminary examination. Figure 6 represents a spall damage evaluation chart derived from the experimental results and numerical simulation, where simplified 2D models were analysed changing the parameters of notch height h and a half wavelength of notch rows y with the intervals of 1 mm and 0.2 mm respectively. The area where the values of y are under numerical critical points for every notch height h represents the notch configuration, where spall failure does not occur. The effect of such slant sur-

FIG. 6. a) A spall damage evaluation chart of explosively loaded V-notched plates with the height of 20 mm for explosives and plates based on the results of this study, and b) – the related configuration parameters of V-notch.

faces comes obviously from weakened interaction of released waves due to the dispersion of directions for reflection waves, but in the area where y is above numerical critical value, the spall failure is inevitable. Especially in the area where y is over the value of 3.4 in the figure, vertical or inner notch ridge spall occurs be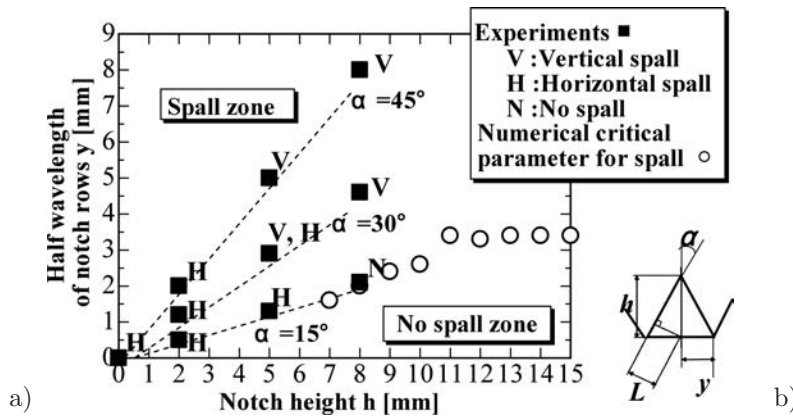cause release waves reflected at the slant surfaces grow enough to spallation. Distance L in (b) is also related with the inner notch ridge failure. On the contrary, in the spall failure area where y is under the value and furthermore notch height h is small, interaction effect of slant surfaces of V-notch rows is diminished and horizontal or ordinary spall occurs.

6. Conclusion

Reduction of spall failure for plates loaded directly by plane detonation wave generator was investigated machining V-notch rows at the free surfaces. Experimental and numerical results revealed remarkable effect of the slant surfaces V-notches, and a notch parameter chart for spall damage evaluation was suggested successfully. The damage reduction method introduced in this study can be applied to explosively loaded plates with other dimensions, in cooperation with numerical simulation. In the future study, more simplified system will be required for the practical use.

References

1. F. Tuler and B. M. Butcher, *Criterion for the Time Dependence of Dynamic Fracture*, International Journal of Fracture Mechanics, **4**, 431–437, 1968.

2. T. Hiroe, K. Fujiwara, Matsuo Hideo, and N, N. Thadhani, *Explosively Produced Spalling in Metals and Its Loading Effects*, Proceedings of the 4th International Symposium on Impact Engineering, A. Chiba, S. Tanimura, and K. Hokamoto [Eds.], Elsevier Science Ltd., Oxford, 851–856, 2001.

3. T. Hiroe, K. Fujiwara, H. Hata, and Y. D. Tsutsumi, *Spall Fracture of Metallic Circular Plates, Vessel Endplates and Conical Frustums Driven by Direct Explosive Loads*, Proceedings of the Conference of the APS Topical Group on Shock Compression of Condensed Matter, M. Elert, M.D. Furnish, R. Chau, N. Holmes and J. Nguyen [Eds.], American Institute of Physics, New York, 537–540, 2007.

4. K. Nakasato, T. Hiroe, K. Fujiwara, H. Hata, *The Effect of Slanting Side Surfaces on the Spall Fracture Behaviour of Metallic Plates Induced by Explosive Shock Waves and Its Application to Novel Plates Structures for Damage Reduction*, Proceedings of International Workshop on Explosion, Shock Wave and Hypervelocity Phenomena 2008, pp. 54–57, Kumamoto University, Kumamoto, 2008.

5. D. J. Steinberg, *Equation of State and Strength Properties of Selected Materials*, LLNL Report UCRL-MA-106439, 1991.

MEASUREMENTS OF STRAIN-RATE DISTRIBUTIONS ON MATERIAL AFTER SHPB IMPACT

M. K a w a i [1], M. F u t a k a w a [2], T. N a o e [2], H. Y a m a d a [3], and C.N. X u [3]

[1] **High Energy Accelerator Research Organization**
Tsukuba, Ibaraki-ken 305-0801, Japan
e-mail: masayoshi.kawai@kek.jp

[2] **J-PARC Center, Japan Atomic Energy Agency**
Tokai-mura, Ibaraki-ken 319-1195, Japan

[3] **National Institute of Advanced Industrial Science and Technology (AIST)**
AIST Kyushu
Tosu, Saga-ken 841-0052, Japan
e-mail: cn-xu@aist.go.jp

We have proposed a sophisticated novel method of the SHPB experiment to measure the local strain-rate distributions on a surface of the specimen by using mechanoluminescent materials combined with a high-speed camera and an image intensifier. The feasibility study was made for the aluminum specimens pasted by a typical mechanoluminescent material -Eu doped $SrAl_2O_4$ film, in order to obtain the fundamental data for the method. Our results showed that $SrAl_2O_4$: Eu emitted lights as a response to the stress. Increase of the light intensity was swift enough to follow the strain change due to SHPB impact. The luminescence intensity was experimentally verified and expressed as a product of strain and strain rate. Accordingly, it can be said that this method gives a good tool for measuring time variation of local strain distributions.

1. Introduction

The Split Hopkinson Pressure Bar (SHPB) technique is widely used to measure a stress-strain relation of materials with a well-controlled impact loading of a specimen. Recently some new SHPB test methods were developed together with analysis by numerical simulations [1, 2] because deformation of the specimen extends the range of elasticity due to very high strain-rate, or specimen of soft materials such as nylon. For new materials of limited quantities, multi-section striker method was developed by combining numerical simulation to save an amount of material to be tested [3]. Various SHPB experiments were

reported for composite materials characterized by non-uniform media [4–6]. Experiments for particle reinforced metal matrix composite (such as SiCp/2024Al composite) showed that composite's strength was weakened by adiabatic heat and cumulative damage under high strain rate compression [4]. Characterization of carbon-fiber reinforced 3D waves was made by tensile loading and shear loading in the SHPB experiments, providing the data for failure and damage behavior [5]. Unidirectional carbon/epoxy laminated composites were investigated to obtain a compressive stress-strain curves up to failure [6].

In the conventional SHPB experiment, strain and strain-rate of a specimen can be calculated from pulse data measured by strain gages mounted on the input and output bars with an assumption of homogeneous deformation of the specimen. Thus, the calculated strain and strain-rate are those of the specimen as a whole. In the case followed by failure and damage, anisotropic 3D and especially local strain, seems to play an important role in crack initiation. Accordingly, in order to analyze the mechanism to the failure and damage due to impact, it will be necessary to measure such local strains. A novel method of photography measuring 3D deformation of the specimen in the SHPB experiments was developed by M.R. ARTHINGTON [7], using a high-speed camera and mirrors. Trial experiment was made on Ti-6Al-4V specimen assuming that material strength was dependent on the rolling direction [8]. The cylindrical specimen was deformed to elliptic with SHPB loading, and major and minor radii of an ellipse were measured by detecting the edge of the image taken by the camera as a function of the axial position and time. The data were compared with the results of a finite element analysis. Spall test of glass-fibre reinforced polymers was also made using a Hopkinson bar configuration together with a high-speed camera [9].

Even in these novel techniques, the local strain can be hardly measured, because it is very difficult for experimentalists to distinguish, with a high accuracy, local deformations from an image caught by the high-speed camera. Additionally, the method to measure the strain-rate has not been reported as yet. The research group of Chao-Nan Xu, one of the authors, has developed a smart material with a property to emit lights the intensity of which is proportional to stresses given to the material, that is called a mechanoluminescence material [10–12]. If we paste a proper mechanoluminescent material on the specimen of the SPHB experiment, it will emit lights corresponding to the strain and strain-rate of the specimen. Accordingly, we will be able to directly obtain the data for strain and strain-rate distributions on the surface of the specimen from the light image, which will be taken by a high-speed camera. In the present work, we have investigated the applicability of the method, by selecting a typical mechanoluminescence material, Eu doped $SrAl_2O_4$ as a sensor of the SPH experiments, to give the time-dependent strain distributions.

2. Experiments

A plane-strain wave incident experiment was carried out using a modified split Hopkinson bar impact technique for aluminum specimens with surfaces pasted by a $SrAl_2O_4$:Eu film, as shown in Table 1. The cylindrical specimen 16 mm high and 8 mm in diameter was placed between the stainless-steel input and output bars of 16 mm in diameter and 1.5 meter in length, as shown in Fig. 1.

Table 1. List of the method of pasting $SrAl_2O_4$:Eu on the aluminum specimen.

Identification	Method
AL-2-F-2	To paste inconel sheet with sputtered $SrAl_2O_4$:Eu
AL-3-G	To paste aluminum film with sprayed $SrAl_2O_4$:Eu
AL-4-3	To spray $SrAl_2O_4$:Eu directly on aluminum specimen
AL-1-3	To paste aluminum film with screen-printed $SrAl_2O_4$:Eu
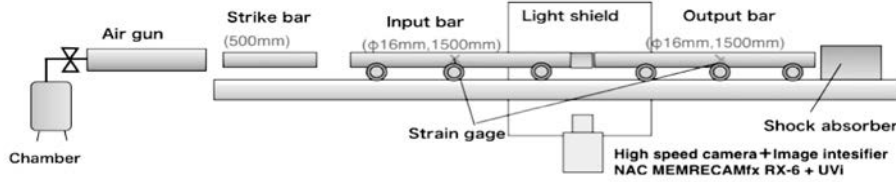
Fig. 1. Schematic of a modified SHPB apparatus.

In a conventional SHPB, an assumption is made that a uniaxial homogeneous stress distribution is produced along the axial direction of the specimen and the forces imposed on both ends of the bars are equal. Then the average nominal strain $\varepsilon(t)$, strain rate $\dot{\varepsilon}(t)$ and stress $\sigma(t)$ in the specimen are obtained from the reflected strain $\varepsilon_r(t)$ and transmitted strain $\varepsilon_t(t)$, measured in the Hopkinson bars as follows:

$$(2.1) \qquad \varepsilon(t) = \frac{-2c_0}{l_s} \int_0^t \varepsilon_r(t')dt',$$

$$(2.2) \qquad \dot{\varepsilon}(t) = \frac{-2c_0}{l_s}\varepsilon_r(t),$$

$$(2.3) \qquad \sigma(t) = \frac{EA}{A_s}\varepsilon_t(t),$$

where A is the cross-sectional area, c_0 the longitudinal elastic wave velocity of the Hopkinson bars, E the Young modulus of the bars, and A_s and l_s are the cross-sectional area and the gage length of the specimen.

Picture of luminescence from $SrAl_2O_4$:Eu after the SHPB impact was taken by a high-speed camera NAC MEMRECAMfx RX-6 with a condition of 20 000 frames per second during 40 μs exposure, by multiplying light intensity with image intensifier NAC UVi.

3. Experimental results and discussions

Initially, impact tests were performed for the same AL-4-3 specimen, characterized by direct spaying, under a condition of loading velocity of the striking bar from 2.66 m/s, 4.10 m/s and 5.32 m/s, by controlling the air pressure in a chamber. Light emission was observed at the loading velocities of 4.10 m/s and 5.32 m/s, while not observed at 2.66 m/s. Accordingly, other specimens were tested at the loading velocity of about 4 m/s and light emission was observed for AL-3-G and AL-1-3. The specimen with inconel film did not shine because of smaller strain due to high modulus of the inconel. Figure 2 shows the pictures at a time when luminescence intensity became the highest. It is found that the luminescence has broad two-dimensional distributions the peak of which appears at the output-bar side from the center of the specimen, except for the case of AL-3-G-002. The case of AL-4-3-003, which had a weak remaining luminescence due to the previous impact test for AL-4-3-002, shows a slightly weaker luminescence in the figure. Dark region in the lower part of a left-hand side (output-bar side) was due to grease fixing the specimen to the experimental apparatus.
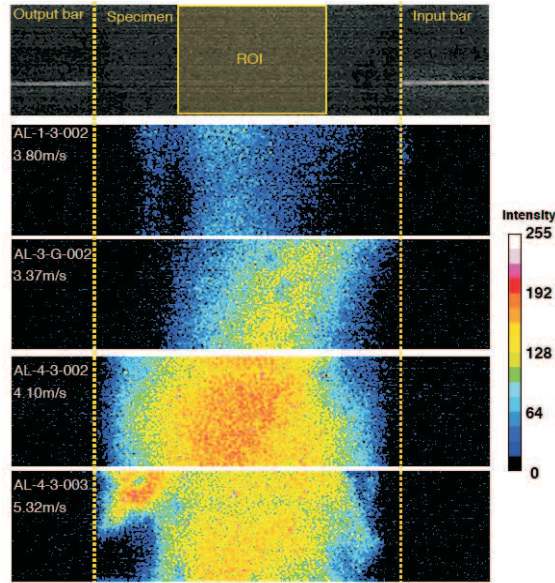
FIG. 2. Picture of peak luminescence.

Figure 3 compares time variation of mean intensity of luminescence among 4 cases. All cases show a quite swift rise-up and decay within 0.5 ms. After that, slow decaying follows over 10 ms. From the figure, it can be said that the method of direct spraying a mechanoluminescence material on the specimen is better than other, because mean intensity of the AL-4-3 specimens are higher than the other specimens.
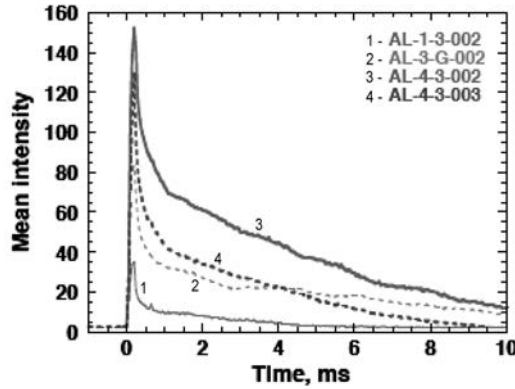
FIG. 3. Time variation of mean intensity of luminescence.

Figure 4 shows the AL-4-3-002 luminescence distribution change with time after the SHPB impact along the central horizontal lines, where the light intensity became the highest. Horizontal distribution is moving, according to movement of the specimen location, towards the output bar. The growing area also changes by getting narrow. These luminescence distribution change will be useful to understand the deformation behaviour of the specimen.
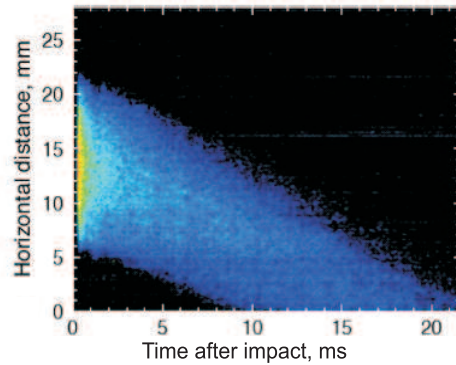
FIG. 4. Luminescence distribution along the central horizontal line.

Figure 5 shows the strain data of ε_i, ε_r and ε_t measured by the strain gages at the input and output bars after the SHPB impact. According to Eq. (2.1),
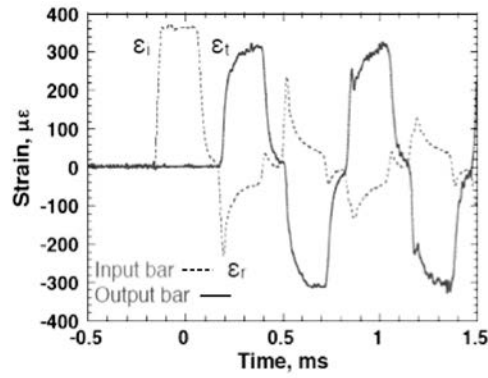
FIG. 5.   Measured strain data.

the strain values of the specimen were calculated as a function of time after the impact. Calculated results compared with luminescence intensity are shown in Fig. 6. In this figure, the relation between the strain and intensity is not obvious in individual cases, even such as made with similar impact loading. The difference must result from different method of pasting $SrAl_2O_4$:Eu on the specimen. Accordingly, it seems to difficult to be derive any quantitative rule between them.
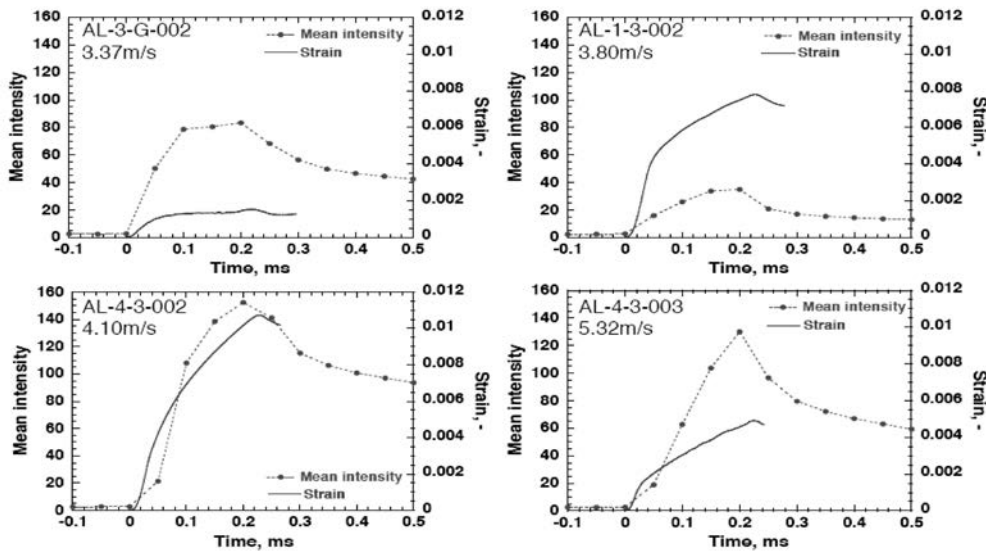
FIG. 6.   Comparison of the strain and luminescence as a function of time.

On the other hand, for cases using the same specimen AL-4-3 it is noted that the latter case AL-4-3-003, even with a larger impact, showed a smaller strain and weaker luminescence than the former case AL-4-3-002. The latter case may be influenced by plastic deformation due to an over-loading beyond elastic

deformation region after the test of the AL-4-3-002. Thus, luminescence may suggest more clearly the type of deformation of the specimen than the strain.

CHAO-NAN XU [11] has derived the following relation between the luminescence intensity and strains:

$$(3.1) \qquad\qquad S_{ML} = C_0 \varepsilon \frac{d\varepsilon}{dt},$$

where, C_0 is the normalization factor.

We applied the above equation, together with Eqs. (2.1) and (2.2), to the case of AL-4-3-002. The calculated luminescence intensity is compared with the experimental one in Fig. 7. Quite good similarity is observed up to the peak at 0.2 ms after the SHPB impact in the figure. This result indicates that the Eq. (3.1) is applicable even to the present swift deformation phenomena.
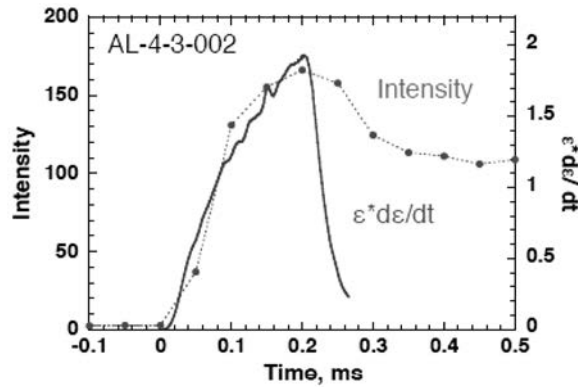
FIG. 7. Comparison of the calculated luminescent intensity with the experimental data.

At a time after the peak, experimental luminescence shows a slow decay. Such decay components are the appearance of an inherent property of the mechano-luminescence materials, and it will be possible to remove the contamination of the remaining luminescence in the pixel-wise from the picture by assuming a decay mode, which can be evaluated at a time properly elapsed from the peak time.

Thus, it can be said that the mechanoluminescence gives us information on the strain phenomena exactly composed of a product of strain and strain rate, and has a possibility to measure a time-dependent local strain distributions. On the other hand, K. ANDERSON [14] has reported the grating technique to measure three-dimensional strain using stereo cameras. The technique is used to determine the three-dimensional deformation and the tangential strain of sheet metal. A grating is fixed on the surface and taken by stereo-cameras in different deformation states. By suitable line-following software, the grating coordinates

in the images are determined with subpixel accuracy. Using photogrammetric methods, the three-dimensional coordinates are calculated from the image coordinates. The strain is usually determined by means of a deformation gradient, which is calculated from every deformed triangle. Thus, we will be able to evaluate the strain-rate by subtracting the effect of the strain data measured with high-speed stereo-cameras from the measured luminescence distributions.

4. Conclusion

We have proposed a sophisticated novel method of the SHPB experiments to measure the local strain-rate distributions by using a mechanoluminescence materials, combined with a high-speed camera and image intensifier. The feasibility study was made for the aluminum specimens with a typical mechanoluminescence material, Eu doped $SrAl_2O_4$ film, in order to obtain the fundamental data for the method. Results showed that $SrAl_2O_4$:Eu emitted lights with response to the strain on the sample surface. The rise of the light intensity was swift enough to follow the strain due to the SHPB impact. It was also verified that the luminescence intensity was expressed as a product of strain and strain-rate, even in the swift deformation such as the SHPB experiments.

Accordingly, the present method can be said to give a good tool to measure local strain-rate distributions by applying a technique to measure the strain displacements with high-speed stereo cameras. Further experiments will be needed to confirm the reliability and to improve the method by selecting a better mechanoluminescence materials, as well as developing a data-acquisition and -processing system, obtaining a local strain distributions in the SHPB experiment. If we manage to develop a more sensitive sensor, swifter phenomena with in microsecond will be also observable by using a suitable high-speed camera and image-intensifier. Wider application will be also possible in the field of mechanical dynamics experiments [13]. The results will clarify the reliability of the fundamental Eqs. (2.1) to (3.1) in the SH'B experiments and the phenomena leading cracks.

Acknowledgment

References

1. L. Wang, H. Lai and J. Zhu, *Studies on high strain-rate behavior of materials by using a new method combining HPB technique with Lagrangian analysis*, Proceedings of the 9th

International Conference on the Mechanical and Physical Behavior of Materials under Dynamic Loading (DYMAT 2009), Vol. 1, pp. 43–49, 2009, ISBN: 978-2-7598-0472-6.

2. T. Umeda and K. Mimura, *Accurate measurement of stress-strain relation under high strain rate condition by using non-coaxial Hopkinson bar method*, ibid., **1**, 127–134, 2009.

3. A. Bouamoul, M. Bolduc and R. Arsenaut, *Development of multi-section striker for split Hopkinson bar experiments and numerical simulation*, ibid., **1**, 149–154, 2009.

4. Y. Zhu, B. Pang, B. Gai, L. Wang and W. Zhang, *Dynamic compressive behavior of 45 col.% SiCp/2024Al composite at various strain rate*, ibid., **1**, 155–161, 2009.

5. R. Gelach, C. R. Siviour, N. Petrinic, and J. Wiegand, *Experimental characterization of the strain rate dependent failure and damage behavior of 3D composite*, ibid., **1**, 219–225, 2009.

6. T. Yokoyama and K. Nakai, *Impact compressive failure of a unidirectional carbon/epoxy laminated composite in three principal material directions*, ibid., **1**, 639–646, 2009.

7. M. R. Arthington, C. R. Siviour, N. Petrinic, and B. C. F. Elliott, *Cross-section reconstruction during uniaxial loading*, Measurement Science and Technology, **20**, 075701, 2009.

8. E. Wielewski, C. R. Siviour, N. Petrinic, M. R. Arthington and S. Carter, *Taylor impact experiments on Ti-6Al-4V specimens using 3D geometry reconstruction and instrumented target rods*, Proceedings of the 9th International Conference on the Mechanical and Physical Behavior of Materials under Dynamic Loading (DYMAT 2009), **1**, 257–263, 2009.

9. R. Govender, L. Louca, A. Pullen and G. Nurick, *High strain rate delamination of glass fibre reinforced polymers using a Hopkinson bar configured for spalling*, ibid., **1**, 449–455, 2009.

10. C. N. Xu, T. Watanabe and M. Akiyama, *Direct view of stress distribution in solid by mechanoluminescence*, App. Phys. Letters, **74**, 2414–2416, 1999.

11. C. N. Xu, *Coating*, [in:] Encyclopedia of SMART Materials, Mel Schwarits [Ed.], John Wiley & Sons, Inc., **1**, 190–201, 2002.

12. C.N. Xu, H. Yamada, X. Wang and X.G. Zheng, *Strong elastico-luminescence from monoclinicstructure $SrAl_2O_4$*, App. Phys. Letters, **84**, 3040–3042, 2004.

13. C. N. Xu, *Sensing technology with elastico-luminescence* [in Japanese], Ceramics Japan, 154–160, 2009.

14. K. Anderson, *Strain tensor for large three-dimensional surface deformation of sheet metal from an object grating*, Experimental Mechanics, **39**, 30–35, 1999.

EVALUATION OF DYNAMIC COMPRESSIVE PROPERTIES OF PLA/PBAT POLYMER ALLOYS USING SPLIT HOPKINSON PRESSURE BAR METHOD

M. N i s h i d a [1]), H. I c h i h a r a [1]), N. F u k u d a [2])

[1]) **Department of Mechanical Engineering, Nagoya Institute of Technology**

Japan

[2]) **Aichi Industrial Technology Institute**

Japan

Poly(lactic acid) (PLA) is a biodegradable biomass polymer. Polymer blends or polymer alloys have been used to overcome its brittleness. Because poly(butylene/adipate/terephthalate) (PBAT) is a ductile and biodegradable polymer, PLA/PBAT polymer alloys can potentially exhibit high impact strengths. Different mixing ratios of PLA/PBAT (80:20, 70:30 and 60:40) and the addition of dialkylperoxide as compatibilizing agent for each mixing ratio have been examined. The stress-strain curves of the PLA/PBAT specimens (observed using a scanning electron microscope) were measured using a split Hopkinson pressure bar (Kolsky bar) and a universal testing machine. The PBAT ratios and addition of dialkylperoxide affected the stress-strain curves. Yield stress decreased with increasing PBAT ratios. Addition of dialkylperoxide did not change the yield stress of specimens when PLA:PBAT = 80:20. At high strain rates, the addition of dialkylperoxide clearly reduced yield stress and Young's modulus when PLA: PBAT = 70:30 and 60:40.

1. INTRODUCTION

The increasing use of plastic products worldwide is causing considerable damage to the environment; therefore, biodegradable plastics (plastics that can decompose in the natural environment) and biomass plastics (plant-derived or recyclable-resource-based plastics) are being extensively investigated, and new biodegradable and biomass plastics are continuously being developed. Poly(lactic acid) (PLA) is a typical biodegradable biomass polymer (plant-derived polymer). In Japan, PLA is already being used to manufacture many industrial products such as the interior parts of cars, parts of computer cases, and cell-phone cases. Many studies have been conducted to determine other industrial products that can be manufactured using PLA. However, such applications are limited to machine parts that are subjected to low loading. Polymer blends/alloys or natural fiber reinforcing have been used to overcome the brittleness of PLA [1–4]. Because poly(butylene adipate / terephthalate) (PBAT) is a ductile and biodegradable polymer, PLA/PBAT polymer blends and alloys can potentially

exhibit high impact strengths [5, 6]. In most cases, the impact resistances of biodegradable plastics and biomass plastics are based only on the experimental results of Izod/Charpy impact strength tests and Dynatup impact tests. However, the basic mechanical properties of such plastics with respect to the impact resistances remain unknown.

In the present study, the stress-strain curves of PLA/PBAT polymer alloys were measured using a universal testing machine and a split Hopkinson pressure bar (Kolsky bar) system. The effects of the mixing ratios of PLA/PBAT and the addition of dialkylperoxide as a compatibilizing agent on the Young's modulus and flow stress were also examined.

2. Experimental methods

2.1. Materials

We used PLA/PBAT alloys prepared by means of PLA from Toyota Motor Corporation (Toyota Eco-Plastic S-17) and PBAT from BASF (Ecoflex). In order to examine the effect of a compatibilizing agent, we used dialkylperoxide (NOF Corporation, PERHEXA 25B). The mixing ratios of PLA and PBAT were 80:20, 70:30, and 60:40. The mixing ratios of PLA:PBAT:dialkylperoxide were 80:20:1, 70:30:1, and 60:40:1. We prepared the polymer alloys using a twin-screw extruder (TECHNOVEL CORPORATION) at 180°C, a screw speed of 400 rpm, and a feed rate of 100 g/min. After melt mixing, the strands prepared by the twin-screw extruder were cooled rapidly, pelletized, and then dried. Next,
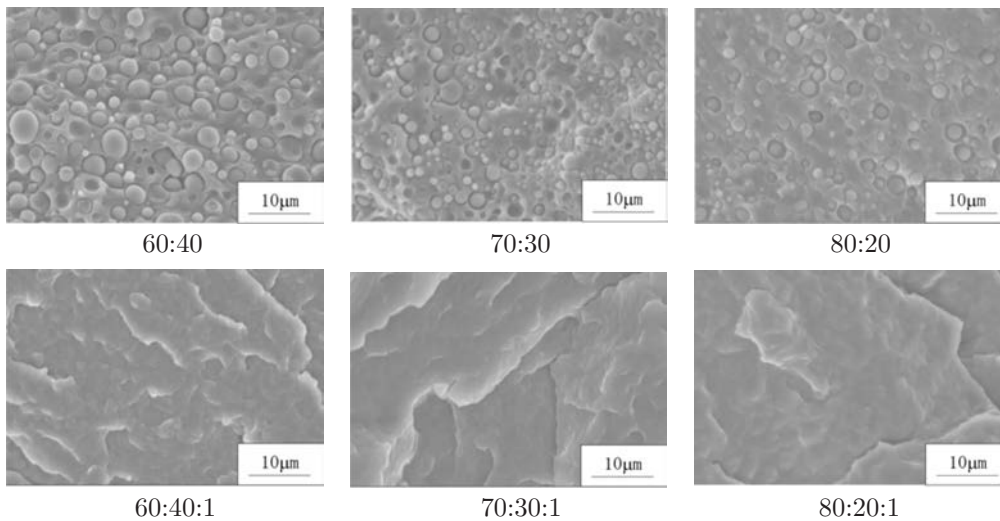
Fig. 1. Photographs of cryo-fractured surfaces (observed using a scanning electron microscope).

5-mm-thick plates were prepared using a conventional hot press at 190°C and 5 MPa for 30 min. Figure 1 shows photographs of the cryo-fractured surfaces of specimens captured using a scanning electron microscope.

In the case of the PLA/PBAT specimens, we can see a sea-island structure consisting of the PLA matrix and PBAT particles of the same size (domain). When we used the compatibilizing agent, we could not observe PBAT particles and phase separation clearly.

2.2. Izod impact tests

Izod impact test specimens were prepared using a milling machine. The specimens had an A-type notch and $63.5 \times 12.7 \times 5$ mm dimensions. An Izod impact testing machine (Toyo Seiki Seisaku-sho, Ltd.) was used.

2.3. Compressive tests

Compressive test specimens were produced using a lathe, and their end faces were polished and parallelized. We used dynamic compressive test specimens with a diameter of approximately 15 mm in order to accurately measure the stress-strain curves using our equipment. The specimen thickness was 5 mm. The photograph of a compressive test specimen is shown in Fig. 2. In the quasi-static tests based on ASTM D695-02a, we used specimens with a diameter and thickness of 6 mm and 9 mm, respectively.
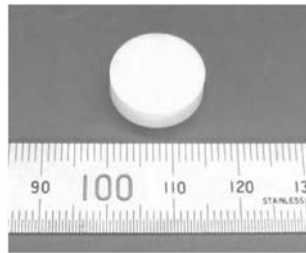
FIG. 2. Photograph of a dynamic compressive test specimen.

The quasi-static compressive tests were conducted with strain rates ranging from 10^{-4} to 10^{-2} s^{-1}, using a universal testing machine (A&D Company, Ltd., RTM-500). At high strain rates of 10^2 to 10^3 s^{-1}, compressive properties of the specimens were examined using the split Hopkinson pressure bar method (Kolsky bar), as shown in Fig. 3. The input and output bars were made of an aluminum alloy (A2024-T4), and their diameters and lengths were 28 mm and 1900 mm/1300 mm, respectively. Strain gages were applied to both sides of the input and output bars at distances of 950 mm and 300 mm from the
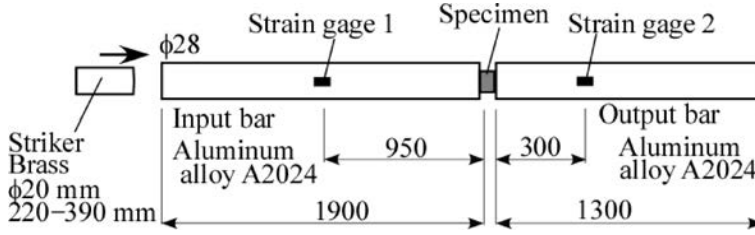
FIG. 3. Experimental setup for split Hopkinson pressure bar method (Kolsky bar).

specimen, respectively. As the stress histories were almost equal on both sides of the specimens, the strain and stress of the specimens were calculated from the strain on the bars using Eqs. (2.1) and (2.2), which are given below; in addition, the strain on the bars was measured using the strain gages [7]:

$$(2.1) \qquad \varepsilon(t) = \frac{2c_3}{L} \int_0^t [\varepsilon_I(t) - \varepsilon_T(t)] \, dt,$$

$$(2.2) \qquad \sigma(t) = \frac{AE}{A_S} \varepsilon_T(t).$$

Here ε_I and ε_T are the axial strains induced in the input bar by the incident wave, and in the output bar by the transmitted wave, respectively. E and c_3 are Young's modulus and elastic wave velocity, respectively, of the both the input and the output bars. L is the specimen thickness. A and A_S are the cross-sectional areas of the input/output bars and specimens, respectively. Material constants of the aluminum alloy (A2024-T4) bars used in the calculations are listed in Table 1. We used brass strikers with a diameter of 20 mm and a length of 220 to 390 mm. During the experiments, the humidity in the laboratory was 15% to 50%. Specimens were maintained at a temperature between 23°C and 25°C using silicone rubber heaters.

Table 1. **Material constants of input and output bars used in calculations.**

Density	Elastic wave velocity in the bar, c_3	Young's modulus E
2.77×10^3 kg/m^3	5150 m/s	73.6 GPa

3. RESULTS AND DISCUSSION

3.1. Results of Izod impact tests

The results of the Izod impact test are shown in Fig. 4. The figure shows the standard deviation of the results and their statistically significant difference. The
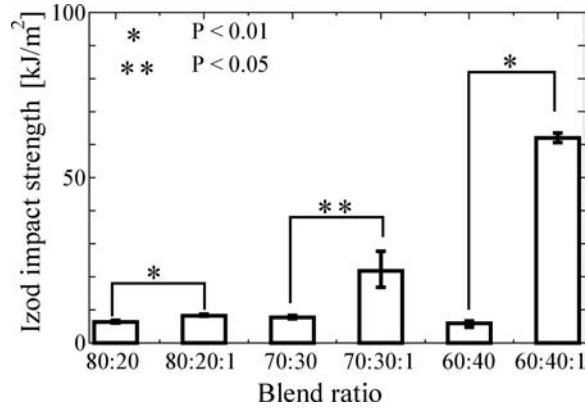
Fig. 4. Impact resistance of different PLA/PBAT alloys.

addition of dialkylperoxide increased Izod impact strength for each PBAT ratio, corroborating the results published by Fukuda et al. [5]. In particular, when the mixing ratio of PLA:PBAT:dialkylperoxide was 60:40:1, the Izod impact strength was 60 kJ/m^2, comparable to polycarbonate (PC).

3.2. Results of compressive tests

The dynamic properties for PLA/PBAT alloy specimens were examined using the split Hopkinson pressure bar method. Figure 5 shows the stress-strain curves for PLA/PBAT alloy specimens, obtained from the strain history and stress history using Eqs. (2.1)–(2.2). Because the strain rate changed slightly during compression, it was determined using the averaged value of the strain rate-strain curve [8]. When PLA:PBAT = 80:20, the stress-strain curve for the specimen peaked near the elastic limit and then, the stress decreased gradually
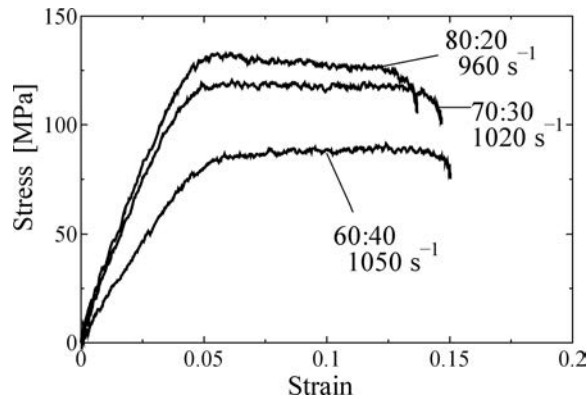
Fig. 5. Effect of PBAT content on stress–strain curves at strain rates of 960–1050 s^{-1}.

with increasing strain (softening). As the PBAT ratio increased, the peak of the stress-strain curve became smaller, and the yield stress and Young's modulus decreased. When PLA:PBAT = 70:30, the flow stress remained almost constant. When PLA:PBAT = 60:40, the flow stress increased slightly (work hardening).

Next, in order to examine the effect of dialkylperoxide addition, the stress-strain curve for PLA:PBAT = 60:40 and PLA:PBAT:dialkylperoxide = 60:40:1 was plotted, as shown in Fig. 6; the curve for PLA:PBAT = 70:30 and PLA:PBAT: dialkylperoxide = 70:30:1 was plotted, as shown in Fig. 7. The addition of dialkylperoxide reduced the yield stress and Young's modulus of the specimens and increased the work hardening.

a) 1050–1090 s^{-1} b) 560–650 s^{-1}
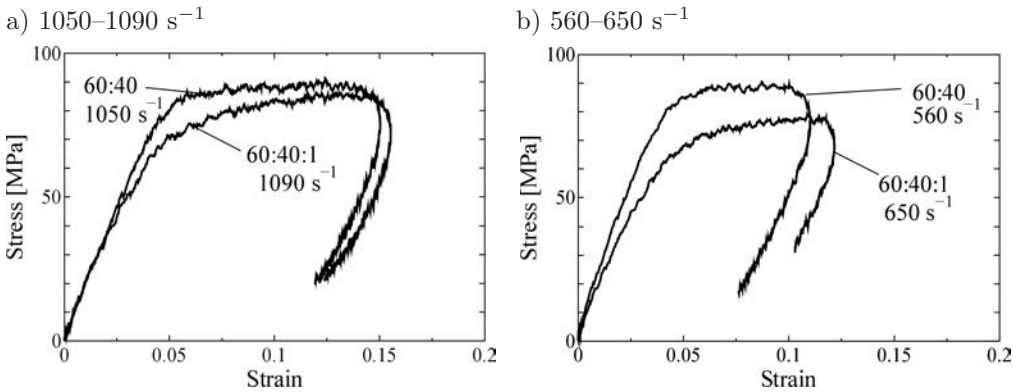
FIG. 6. Effect of dialkylperoxide addition on the stress-strain curve for PLA:PBAT = 60:40 and PLA:PBAT:dialkylperoxide = 60:40:1.

a) 990–1020 s^{-1} b) 750–790 s^{-1}
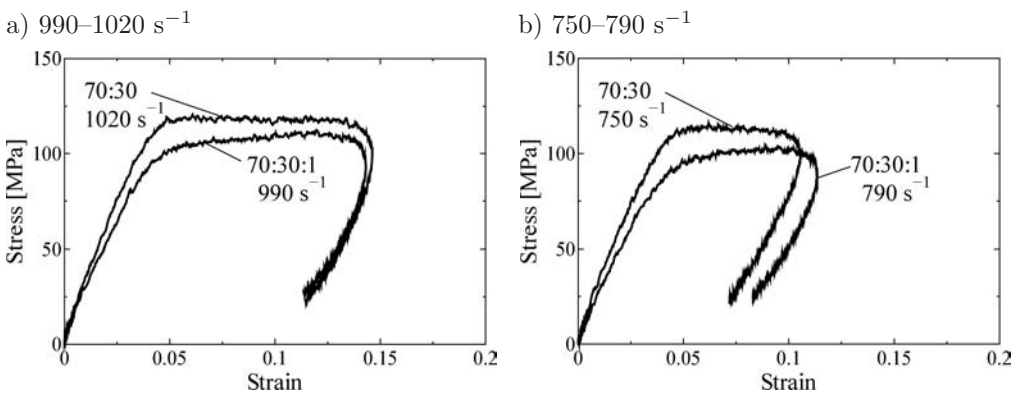
FIG. 7. Effect of dialkylperoxide addition on stress-strain curve for PLA:PBAT = 70:30 and PLA:PBAT:dialkylperoxide = 70:30:1.

Finally, Fig. 8 shows the effect of the strain rate on the yield stress. For each polymer alloy, the yield stress increased with the strain rate, what is commonly seen in most engineering plastics such as poly(methyl methacrylate) (PMMA)
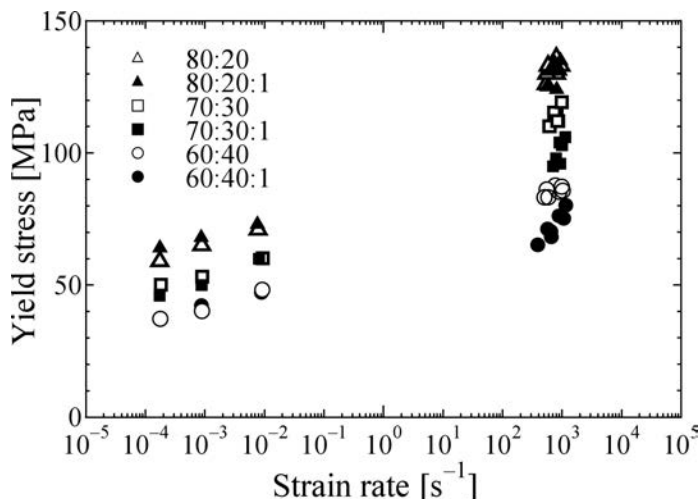
Fig. 8. Effect of strain rate on maximum stress.

and PC. As the PBAT ratio increased, the yield stress decreased at high and low strain rates. At low strain rates, we can see only a few effects of dialkylperoxide addition on the yield stress for each PBAT ratio. At high strain rates, the addition of dialkylperoxide clearly reduced the yield stress only for PLA: PBAT = 70:30 or 60:40. The strain rate dependence of the yield stress was greater when PLA:PBAT: dialkylperoxide = 70:30: 1 and 60:40:1 than when PLA:PBAT = 70:30 and 60:40.

4. Conclusions

We have examined specimens with different mixing ratios of PLA/PBAT and the effect of the addition of dialkylperoxide on them. The addition of dialkylperoxide increased the Izod impact strength. The stress-strain curves of PLA/PBAT specimens were measured using a split Hopkinson pressure bar and a universal testing machine. The yield stress and Young's modulus decreased with increasing PBAT ratios. At high strain rates, when PLA:PBAT = 70:30 and 60:40, the addition of dialkylperoxide reduced the yield stress and Young's modulus, and increased the work hardening. The strain rate dependence of the yield stress was greater when PLA:PBAT: dialkylperoxide = 70:30:1 and 60:40:1 than when PLA:PBAT = 70:30 and 60:40.

Acknowledgment

References

1. H. Tsuji, Y. Ikada, *Blends of Aliphatic Polyesters. 1. Physical Properties and Morphologies of Solution-cast Blends from Poly(DL-lactide) and Poly(epsilon- caprolactone)*, Journal of Applied Polymer Science, **60**, 13, 2367–2375, 1996.

2. C.-C. Chen, J.-Y. Chueh, H. Tseng, H.-M. Huang, S.-Y. Lee, *Preparation and Characterization of Biodegradable PLA Polymeric Blends*, Biomaterials, **24**, 1167–1173, 2003.

3. M. Todo, S.-D. Park, T. Takayama, K. Arakawa, *Fracture Micromechanisms of Bioabsorbable PLLA/PCL Polymer Blends*, Engineering Fracture Mechanics, **74**, 12, 1872–1883, 2007.

4. M. Nishida, M. Yamaguchi, M. Todo, T. Takayama, H.-Å Häggblad, P. Jonsén, *Evaluation of Dynamic Compressive Properties of PLA Polymer Blends Using Split Hopkinson Pressure Bar*, [in:] Proceedings of DYMAT 2009, **1**, 909–915, 2009.

5. N. Fukuda, H. Matsubara, R. Kitagawa, *The Crystallization Behaviors and Mechanical Properties of Poly(lactic acid)/Poly(butylenes adipate terephthalate) Alloys*, [in:] Proceedings of 59th Symposium on Macromolecules, pp. 5657–5658, 2007 (in Japanese).

6. F. Signori, M.-B. Coltelli, S. Bronco, *Thermal Degradation of Poly(lactic acid) (PLA) and Poly(butylenes adipate-co-terephthalate) (PBAT) and Their Blends Upon Melt Processing*, Polymer Degradation and Stability, **94**, 74–82, 2009.

7. G. T. Gray III, *Classic Split Hopkinson Pressure Bar Testing*, [in:] ASM Handbook Vol. 8, Mechanical Testing and Evaluation, ASM, 462–476, 2000.

8. K. Nakai, T. Yokoyama, *Strain Rate Dependence of Compressive Stress-Strain Loops of Several Polymers*, Journal of Solid Mechanics and Materials Engineering, **2**, 4, 557–566, 2008.

ELASTIC ENERGY DECOMPOSITION AND LIMIT CRITERIA

J. R y c h l e w s k i

In memoriam Wacław Olszak

1. A bit of history

Exactly 80 years ago[1], in one little known engineering journal, appeared a paper by a young scientist – "*Właściwa praca odkształcenia jako miara wytężenia materiału*" [*Specific work of strain as a measure of material effort* M.T. Huber [1]]. The author's destiny was to become in future a founder of the Polish school of solid deformable bodies mechanics. The article contained one of the classic assertions of contemporary mathematical theory of plasticity – the limit condition for isotropic bodies, which we nowadays use to express as

$$(1.1) \qquad\qquad \mathbf{s} \cdot \mathbf{s} \leq 2k^2,$$

where $\mathbf{s}$ is a deviatoric part of the stress tensor $\boldsymbol{\sigma}$, k denotes the limit value of pure shear stress (the notation is specified in Appendix 1).

We should notice that condition (1.1), gained popularity in scientific environment only ten years later being rediscovered by R. von Mises [2], and subsequently, additionally explained by H. Hencky [3]. This story has been discussed in 1924 at the I-st International Congress of Applied Mechanics in Delft, and found a reflection in, perhaps the first, methodical elucidation of the mathematical theory of plasticity given in 1927 by H. Mierzejewski [4].

After another decade it become clear that the yield condition (1.1) was clearly formulated by J.C. Maxwell in a private letter to prospect lord Kelvin [5]. After the explanation of the matter of the problem, the author of the letter additionally asserts: "*I think this notion will bear working out into a mathematical*

---

[1] Written in 1984.

theory of plasticity when I have time ... ". It is a pity, that such a chance did not come about, we should remember however, that Maxwell's attention has turned to more important problems.

The mentioned above co-authors of the condition (1.1), (except for R. von Mises) based it on the charming in their simplicity, considerations on the energy. Let us recall the matter of the problem.

In a linearly elastic body under small strain $\boldsymbol{\varepsilon}$, the stored elastic energy is equal to the work performed by the stress $\boldsymbol{\sigma}$ on the strain $\boldsymbol{\varepsilon}$ and can be expressed as a quadratic form of stresses,

$$(1.2) \qquad \Phi(\boldsymbol{\sigma}) \equiv \frac{1}{2}\boldsymbol{\sigma} \cdot \boldsymbol{\varepsilon}(\boldsymbol{\sigma}).$$

If a body is isotropic, then this form should be invariant. Any **quadratic invariant** of the symmetric tensor, however, can be expressed as follows:

$$(1.3) \qquad \Phi(\boldsymbol{\sigma}) = A\sigma^2 + B\mathbf{s} \cdot \mathbf{s},$$

where

$$(1.4) \qquad \boldsymbol{\sigma} = \sigma\mathbf{1} + \mathbf{s}, \qquad \sigma \equiv \frac{1}{3}\mathbf{1} \cdot \boldsymbol{\sigma}.$$

Indeed, σ, $\mathbf{s} \cdot \mathbf{s}$ and $\det \mathbf{s}$ comprise a complete (both functional and polynomial) system of invariants on the space of symmetric tensors $\mathscr{S}$, and (1.3) is the only possible quadratic expression which can be created using them. Giving a meaning to the constants, one obtains:

$$(1.5) \qquad \Phi(\boldsymbol{\sigma}) = \frac{1}{2K}\sigma^2 + \frac{1}{4G}\mathbf{s} \cdot \mathbf{s},$$

where K – compressibility modulus, G – shear modulus. It means that

$$(1.6) \qquad \Phi(\sigma\mathbf{1} + \mathbf{s}) = \Phi(\sigma\mathbf{1}) + \Phi(\mathbf{s}),$$

i.e. the elastic energy is the sum of the **energy of the volume change** $\Phi(\sigma\mathbf{1})$ and the **energy of the shape change** $\Phi(\mathbf{s})$. Having performed this decomposition, J.C. Maxwell wrote: "*I have strong reasons for believing, that when $\Phi(\mathbf{s})$ reaches a certain limit..., then the element will begin to give way. ... Condition of not yielding*

$$(1.7) \qquad \frac{1}{h}\Phi(\mathbf{s}) \leq 1,$$

where $h \equiv k^2/2G$. We took the liberty to change only the author's notation for the sake of similarity of the expressions (1.7) and (1.1).

Arising in that place and at that time (Cambridge, middle of the XIX century) of the ideas about the limit capacity of the elastic body for cumulating the energy of shape change seems to us by no means accidental. Some years earlier, one of the professors of that university, J. Green, laid the notion of the elastic energy in the foundations of the very definition of the elasticity [6]; J.G. Stokes pointed out quite clearly on the two kinds of the elasticity: the one trying to restore the volume, and another one tending to restore the shape [7].

M.T. Huber quotes the decomposition (1.6) referring to H. HELMHOLTZ [8] and writes: "*. . . można z wielkim prawdopodobieństwem uważać Φ(s) za miarę wytężenia materiału*" [1] ["*. . . one can in all probability consider Φ(s) as a measure of material effort*" – p. 185, [1] (English translation)]. He communicated his supposition to A. Föppl, who wrote in his well-known at that time textbook [9]: ["*Endlich ist noch darauf hinzuweisen, daß mit den bisher genannten noch keineswegs alle Möglichkeiten erschöpft sind, die für die Bemessung der Bruchgefahr von vornherein offen stehen. Es ist auch sehr wohl möglich, daß wenigstens für gewisse Stoffe eine dieser anderen Möglichkeiten dem wirklichen Verhalten near kommt als die früheren. Namentlich liegt es nahe, in irgendeiner Weise die bezogene Formänderungsarbeit mit der Anstrengung des Stoffes in Verbindung zu bringen, da in ihr sowohl die auftretenden Spannungen als die von ihnen hervorgerufene Formänderung zur Geltung kommen*"].

"*In der Tat hat man dies wiederholt versucht, und eine besondere Form dieser Annahme, die von Herrn Professor Huber an der Technischen Hochschule in Lemberg aufgestellt wurde, erscheint durchaus beachtenswert, weshalb hier noch etwas näher darauf eingegangen werden soll. Die ursprüngliche Veröffentlichung von Huber ist uns nicht zugänglich, da sie in der polnischen Muttersprache ihres Verfassers geschrieben ist; wir können uns aber nach einer brieflichen Mitteilung mit einem ausführlichen Auszuge aus der Abhandlung richten, die wir Herrn Huber verdanken*" [p. 50 [9] (*Finally, one should mention that the before discussed measures of the risk of fracture by no means exhaust all possibilities that are at our disposal. It is also very possible that at least for certain materials one of the other possibilities approximates better the real behaviour than the earlier ones. It is namely conceivable to relate in some way the derived [specific] work of strain with material effort as well as to arrive at the assessment of induced stresses and the resulting deformation.*

In fact one has it repeatedly attempted and certain particular form of such an approach, which was exhibited by Professor Huber of the Technical University in Lemberg [Lwów Polytechnic] appears entirely worthy of our attention. Therefore, it should be brought closer here. The original publication of Huber is not accessible for us, for it was written in Polish mother tongue of the author. However, we can be guided by the comprehensive excerpt by letter, which we owe to Mr Huber.) – translation by sc. ed.].

R. von Mises proposed condition (1.1) starting from purely formal scheme of the quadratic approximation of the Tresca-Saint Venant yield condition. But as soon as the quadratic form is proposed, and a body is isotropic, then the limit function assumes form (1.3) and, discarding the influence of the hydrostatic pressure, one obtains (1.1), i.e. (1.7).

For completeness of the image we should mention, that E. BELTRAMI in 1885 [10] proposed boundedness of the complete elastic energy $\Phi(\sigma)$ as a limit criterion. This proposition was repeated later by B.P. HAIGH [11]. Another old presumptions concerning the limit conditions one can find in the surveys by W. BURZYŃSKI [12] and M.M. FILONENKO–BORODICH [13].

Comment: as it is known, the condition (1.1) can be for isotropic body also differently interpreted. Particularly, V.V. NOVOZHILOV [14] found, that the term $\mathbf{s} \cdot \mathbf{s}$ is proportional to the, averaged over all planes, square of the shear stress value.

2. STATEMENT OF THE PROBLEM

According to the traditions of the old papers, we believe that it is justified, at a certain stage of the knowledge, to consider the form of **limit criterion**, understood as the bounding imposed on some **measure of the stress intensity** (called by M.T. Huber *miara wytężenia* [*material effort*]), without specifying the origins of the "element failure". The last can mean the transition to nonlinear elasticity, arising of permanent deformations (plastic, viscous, viscoplastic), disintegration on the micro- or macro-level, destruction of the composite structure configuration, attaining intolerable extent of deformation and so on.

Nowadays we know, more than the old time masters did, about the mechanisms of numerous effects. However in the same time, the following facts of the matter remain essential. Firstly: all the time increases the manifold of the engineering materials: of alloys, polymers, ceramics, concrete, composites, working mechanisms of their structures remaining as a rule inadequately recognized. Frequently thorough studies on them would be costly and time-consuming. Secondly: essentially, different structural effects can on the macro-level materialize quite similarly. For example, small strain crystal elasticity and elasticity of the solid polymers are based on quite different structural mechanisms, but their "macro-scale output" is identical. From there, the actuality and necessity of the phenomenological approach in the framework of the rational mechanics of materials comes out. Particularly, this remains true with respect to the limit criteria under consideration.

In this context, a phenomenological condition (1.7), for which the choice of the stress intensity measure is based on the fundamental notion of physics – a concept of energy, preserves in our opinion its heuristic attractiveness. *Basing*

on this start point, we set as our task, in the present paper, a comprehensive, from the formal viewpoint, clarification of the possibilities of direct generalization of the energy-based Maxwell–Huber condition (1.7) on linearly elastic anisotropic bodies of arbitrary symmetry.

3. On the answer given by W. Olszak and W. Urbanowski

It seems to be evident, that the first attempt to enlighten the posed problem was taken by successors of M.T. Huber. My tutors, W. Olszak and W. Urbanowski proceeded on the way of extracting from the complete elastic energy of some its part, being an analogue of the energy of the shape change in isotropic body [15]. This study was continued lastly by J. Ostrowska in the lecture devoted to the memory of W. Olszak [16].

Let us consider an arbitrary elastic body described by the quadratic elastic potential

$$(3.1) \qquad \Phi \equiv \frac{1}{2}\boldsymbol{\sigma} \cdot \boldsymbol{\varepsilon} = \frac{1}{2}\boldsymbol{\sigma} \cdot \mathbf{S} \cdot \boldsymbol{\sigma} = \frac{1}{2}\boldsymbol{\varepsilon} \cdot \mathbf{C} \cdot \boldsymbol{\varepsilon}.$$

Here $\mathbf{S}$ is a **compliance tensor**, $\mathbf{C}$ – **stiffness tensor**,

$$(3.2) \qquad \mathbf{C}^T = \mathbf{C}, \qquad \mathbf{S}^T = \mathbf{S}, \qquad \mathbf{C} \circ \mathbf{S} = \mathbf{S} \circ \mathbf{C} = \mathbf{I}$$

(see Appendix 1). From there, in virtue of Hooke's law, it follows:

$$\boldsymbol{\sigma} = \partial_\varepsilon \Phi = \mathbf{C} \cdot \boldsymbol{\varepsilon},$$

$$(3.3)$$

$$\boldsymbol{\varepsilon} = \partial_\sigma \Phi = \mathbf{S} \cdot \boldsymbol{\sigma}.$$

The idea suggested in [15] is attractive mainly because of its stimulating difficulties. Let us try to accomplish it with the aid of the standard decomposition (1.4). Unfortunately, this *does not lead* to the decomposition of the elastic energy. One has:

$$(3.4) \quad \Phi(\boldsymbol{\sigma}) = \frac{1}{2}(\sigma\mathbf{1} + \mathbf{s}) \cdot \mathbf{S} \cdot (\sigma\mathbf{1} + \mathbf{s}) = \frac{1}{2}\sigma^2 \mathbf{1} \cdot \mathbf{S} \cdot \mathbf{1} + \sigma\mathbf{1} \cdot \mathbf{S} \cdot \mathbf{s} + \frac{1}{2}\mathbf{s} \cdot \mathbf{S} \cdot \mathbf{s}.$$

The first term

$$(3.5) \qquad \frac{1}{2}\sigma^2 \mathbf{1} \cdot \mathbf{S} \cdot \mathbf{1} = \Phi(\sigma\mathbf{1}) \geq 0$$

describes the work of hydrostatic pressure $\sigma\mathbf{1}$ on the evoked by this stress state deformation $\sigma\mathbf{S} \cdot \mathbf{1}$, while the last one

$$(3.6) \qquad \frac{1}{2}\mathbf{s} \cdot \mathbf{S} \cdot \mathbf{s} = \Phi(\mathbf{s}) \geq 0$$

represents the work of the deviatoric part $\mathbf{s}$ on the deformation caused by it $\mathbf{S} \cdot \mathbf{s}$. However,

$$(3.7) \qquad \Phi(\boldsymbol{\sigma}) \neq \Phi(\sigma\mathbf{1}) + \Phi(\mathbf{s}),$$

since there exists an additional term, which depends both on σ and $\mathbf{s}$

$$(3.8) \qquad \sigma\mathbf{1} \cdot \mathbf{S} \cdot \mathbf{s},$$

representing the sum of the work of $\sigma\mathbf{1}$ on the deformation $\mathbf{S} \cdot \mathbf{s}$ and, equal to it, work of $\mathbf{s}$ on the deformation $\sigma\mathbf{S} \cdot \mathbf{1}$. Let us notice that $\mathbf{1} \cdot \mathbf{S} \cdot \mathbf{s}$ describes a change of volume generated by the deviatoric part of load $\mathbf{s}$; it can be positive or negative depending on the sign of $\mathbf{s}$. An example of the case of pure shear is shown in Fig. 1. Difference $\Phi(\boldsymbol{\sigma}) - \Phi(\mathbf{s})$ *does not represent* energy of any stress state and it can assume negative values. Thus the use of $\Phi(\mathbf{s})$ as a measure of stress intensity appears out in general to be unsatisfactory.
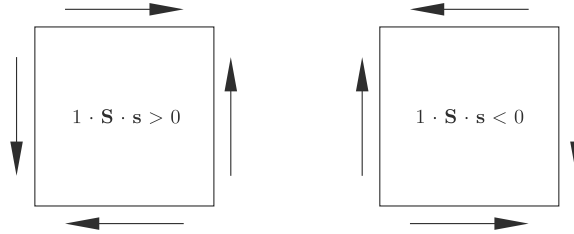
FIG. 1. Volume change $\mathbf{1} \cdot \mathbf{S} \cdot \mathbf{s}$ under the deviatoric load $\mathbf{s}$ depends on the orientation of $\mathbf{s}$ with respect to the elastic body.

Let us try to proceed on another way. We shall decompose the strain tensor

$$(3.9) \qquad \boldsymbol{\varepsilon} = \varepsilon\mathbf{1} + \mathbf{e}, \qquad \varepsilon \equiv \frac{1}{3}\mathbf{1} \cdot \boldsymbol{\varepsilon}$$

and represent the elastic energy as follows:

$$(3.10) \qquad \Phi(\boldsymbol{\sigma}) = \Phi_v(\boldsymbol{\sigma}) + \Phi_f(\boldsymbol{\sigma}),$$

where

$$(3.11) \qquad \Phi_v(\boldsymbol{\sigma}) \equiv \frac{1}{2}\boldsymbol{\sigma} \cdot \mathbf{e} = \frac{1}{2}\mathbf{s} \cdot \mathbf{e} = \frac{1}{2}\mathbf{s} \cdot \mathbf{S} \cdot \mathbf{s} + \frac{1}{2}\sigma\mathbf{1} \cdot \mathbf{S} \cdot \mathbf{s},$$

$$(3.12) \qquad \Phi_f(\boldsymbol{\sigma}) \equiv \frac{1}{2}\boldsymbol{\sigma} \cdot (\varepsilon\mathbf{1}) = \frac{3}{2}\sigma\varepsilon = \frac{1}{2}\sigma^2\mathbf{1} \cdot \mathbf{S} \cdot \mathbf{1} + \frac{1}{2}\sigma\mathbf{1} \cdot \mathbf{S} \cdot \mathbf{s}.$$

Term $\Phi_f(\boldsymbol{\sigma})$ is equal to *the work of the stress $\boldsymbol{\sigma}$ on the shape change*, while $\Phi_v(\boldsymbol{\sigma})$ represents *the work of the stress $\boldsymbol{\sigma}$ on the volume change*. In general, one

can choose load $\boldsymbol{\sigma}$ in such a way, that one of the pair of terms $\Phi_f(\boldsymbol{\sigma})$ and $\Phi_v(\boldsymbol{\sigma})$ becomes negative, while total energy $\Phi(\boldsymbol{\sigma})$ remains positive. Neither $\Phi_f(\boldsymbol{\sigma})$ nor $\Phi_v(\boldsymbol{\sigma})$ represents an elastic energy of any state of stress. Thus $\Phi_f(\boldsymbol{\sigma})$ can not be used as a measure of stress intensity [material effort].

Let us notice that these difficulties disappear with vanishing of the term (3.8), i.e. for the elastic bodies fulfilling the condition

$$(3.13) \qquad\qquad \mathbf{1} \cdot \mathbf{S} \cdot \mathbf{s} = 0,$$

for all deviatoric tensors $\mathbf{s}$.

This condition was, perhaps for the first time, proposed by the student of M.T. HUBER – W. BURZYŃSKI [12]. In his opinion, it could turn up to obey in general for all elastic bodies and to replace the famous A. CAUCHY condition [17], which evoked vigorous disputes in XIX century [18]. This is not true, of course. In [19] we have called the bodies obeying (3.13) *volumetrically-isotropic*. Condition (3.13) means that the hydrostatic load produces only volumetric deformation.

$$(3.14) \qquad\qquad \begin{aligned} \mathbf{S} \cdot \mathbf{1} &= \frac{1}{3K}\mathbf{1}, \\[2mm] \frac{1}{K} &\equiv \mathbf{1} \cdot \mathbf{S} \cdot \mathbf{1}, \end{aligned}$$

i.e. the unit tensor $\mathbf{1}$ is a **proper elastic state**. Isotropic bodies are volumetrically-isotropic, because in this case

$$(3.15) \qquad\qquad \mathbf{S} = \frac{1}{3K}\mathbf{I}_{\mathscr{P}} + \frac{1}{2G}\mathbf{I}_{\mathscr{D}},$$

where

$$(3.16) \qquad\qquad \mathbf{I}_{\mathscr{P}} \equiv \frac{1}{3}\mathbf{1} \otimes \mathbf{1}, \qquad \mathbf{I}_{\mathscr{D}} \equiv \mathbf{I} - \frac{1}{3}\mathbf{1} \otimes \mathbf{1}$$

and (3.13) holds since $\mathbf{I}_{\mathscr{P}} \cdot \mathbf{1} = \mathbf{1}$, $\mathbf{I}_{\mathscr{D}} \cdot \mathbf{1} = \mathbf{0}$ [19][2].

Let us come back however to the general case, when (3.13) does not hold. The authors of [15] passed over one idea which flashed across the thesis [12] (see p. 30), written under direct supervision of M.T. Huber. W shall attribute, for the beginning, a necessary clearness to this idea. Let us consider, beginning from this point, the stress $\boldsymbol{\sigma}$ as being related to some standard one and hence, being

---

[2]Obviously, (3.13) is fulfilled for any incompressible material, since in this case $\mathbf{1} \cdot \mathbf{S} \cdot \boldsymbol{\sigma} = 0$ for any stress tensor $\boldsymbol{\sigma}$. Such a case is (from the formal viewpoint) not covered by equalities (3.14) (Translator's remark).

dimensionless. This enables us to consider $\boldsymbol{\sigma}$ and $\boldsymbol{\varepsilon}$ as elements of the space of symmetric tensors $\mathscr{S}$.

Definition. Two stress states $\boldsymbol{\alpha}$, $\boldsymbol{\beta}$ we shall call **energy-separated** for a given elastic body, if they decompose its elastic energy, i.e. if

$$(3.17) \qquad \Phi(\boldsymbol{\alpha} + \boldsymbol{\beta}) = \Phi(\boldsymbol{\alpha}) + \Phi(\boldsymbol{\beta}).$$

Two subspaces $\mathscr{A}$, $\mathscr{B}$ in $\mathscr{S}$ we shall call energy-separated if all pairs $\alpha \in \mathscr{A}$ and $\beta \in \mathscr{B}$ are energy-separated. The first example of the energy-separation is already known to us: for every isotropic linearly-elastic body, a one-dimensional space of spherical tensors $\mathscr{P}$ and five-dimensional space of deviators $\mathscr{D}$

$$(3.18) \qquad \mathscr{S} = \mathscr{P} \oplus \mathscr{D},$$

are energy-separated according to (1.6).

We have not assumed in our definition that a body is linearly-elastic, we should mention however that utility of the introduced notion in general case is rather doubtful. In the case of linearity, though it works excellently, as we shall make evident. Here

$$(3.19) \qquad (\boldsymbol{\alpha} + \boldsymbol{\beta}) \cdot \mathbf{S} \cdot (\boldsymbol{\alpha} + \boldsymbol{\beta}) = \boldsymbol{\alpha} \cdot \mathbf{S} \cdot \boldsymbol{\alpha} + \boldsymbol{\beta} \cdot \mathbf{S} \cdot \boldsymbol{\beta} + 2\boldsymbol{\alpha} \cdot \mathbf{S} \cdot \boldsymbol{\beta}$$

and the energy-separation condition takes the form

$$(3.20) \qquad \boldsymbol{\alpha} \cdot \mathbf{S} \cdot \boldsymbol{\beta} = \boldsymbol{\beta} \cdot \mathbf{S} \cdot \boldsymbol{\alpha} = 0.$$

Thus, for the case of linear elasticity, *energy-separation of* $\boldsymbol{\alpha}$ *and* $\boldsymbol{\beta}$ *means that the stress* $\boldsymbol{\alpha}$ *does not perform work on the strain caused by the stress* $\boldsymbol{\beta}$, and equally: $\boldsymbol{\beta}$ does not work on $\mathbf{S} \cdot \boldsymbol{\alpha}$.

Now, everything is ready for a description of the following simple case. Assume that, for the class of elastic bodies under consideration, there exists such a tensor $\boldsymbol{\alpha}$, that the stress $c\boldsymbol{\alpha}$ of any intensity c does not cause a failure of the element (in the particular sense under consideration). We shall call the states $c\boldsymbol{\alpha}$ **the safe** ones. They constitute a one-dimensional space

$$(3.21) \qquad \mathscr{E} \equiv \{c\boldsymbol{\alpha} \mid c: \text{ arbitrary number}\}.$$

Let us introduce its orthogonal complement

$$(3.22) \qquad \mathscr{E}^{\perp} \equiv \{\boldsymbol{\beta} \mid \boldsymbol{\beta} \cdot \boldsymbol{\alpha} = 0\}.$$

We choose now *all states energy-separated from* $\boldsymbol{\alpha}$. They constitute a five-dimensional space

$$(3.23) \qquad \mathscr{E}^{\dot{\perp}} \equiv \{\boldsymbol{\omega} \mid \boldsymbol{\omega} \cdot \mathbf{S} \cdot \boldsymbol{\alpha} = 0\}.$$

Evidently

$$(3.24) \qquad \mathscr{E}^{\dot{\perp}} = \mathbf{C} \cdot \mathscr{E}^{\perp} = \{\mathbf{C} \cdot \boldsymbol{\beta} \mid \boldsymbol{\beta} \cdot \boldsymbol{\alpha} = 0\}.$$

The state $\boldsymbol{\alpha}$ is a normal of $\mathscr{E}^{\perp}$ while the state $\mathbf{S} \cdot \boldsymbol{\alpha}$ is a normal of $\mathscr{E}^{\dot{\perp}}$, Fig. 2.
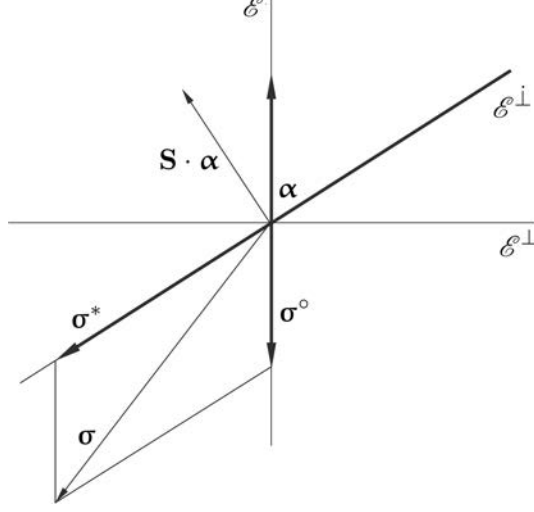
FIG. 2. $\mathscr{E}$ – space of safe states, $\mathscr{E}^{\dot{\perp}}$– space of the states energy-separated from the safe ones, $\mathscr{E}^{\perp}$ – space of the states orthogonal to the safe states.

Let us introduce a decomposition into a direct sum

$$(3.25) \qquad \mathscr{S} = \mathscr{E} \oplus \mathscr{E}^{\dot{\perp}}$$

i.e. we shall represent every stress $\boldsymbol{\sigma}$ as a sum of energy-separated parts, the first of them being a safe state

$$(3.26) \qquad \boldsymbol{\sigma} = \boldsymbol{\sigma}^{\circ} + \boldsymbol{\sigma}^{*}, \qquad \boldsymbol{\sigma}^{\circ} \in \mathscr{E}, \qquad \boldsymbol{\sigma}^{*} \in \mathscr{E}^{\dot{\perp}}.$$

The component $\boldsymbol{\sigma}^{\circ}$ will be called the **safe part** of the stress $\boldsymbol{\sigma}$, and the component $\boldsymbol{\sigma}^{*}$ – **the hazardous** one. Making use of the condition of energy-separation $\boldsymbol{\sigma}^{\circ} \cdot \mathbf{S} \cdot (\boldsymbol{\sigma} - \boldsymbol{\sigma}^{\circ}) = 0$, one obtains

$$(3.27) \qquad \boldsymbol{\sigma}^{\circ} = \sigma^{\circ}\boldsymbol{\alpha}, \qquad \sigma^{\circ} \equiv \frac{\boldsymbol{\alpha} \cdot \mathbf{S} \cdot \boldsymbol{\sigma}}{\boldsymbol{\alpha} \cdot \mathbf{S} \cdot \boldsymbol{\alpha}}.$$

Operation $\boldsymbol{\sigma} \to \boldsymbol{\sigma}^{\circ}$ is a projection, parallel with respect to the space $\mathscr{E}^{\dot{\perp}}$, on the straight line $\mathscr{E}$. It is performed with the aid of projector $\mathbf{E}^{\circ} \in \mathscr{T}$, which is uniquely defined as follows:

$$(3.28) \qquad \mathbf{E}^{\circ} \cdot \boldsymbol{\sigma} = \boldsymbol{\sigma}^{\circ} \qquad \text{for all} \qquad \boldsymbol{\sigma} \in \mathscr{S}.$$

It is not difficult to show that the projector $\mathbf{E}^\circ$ is equal to

$$(3.29) \qquad \mathbf{E}^\circ = \frac{1}{\boldsymbol{\alpha} \cdot \mathbf{S} \cdot \boldsymbol{\alpha}} \boldsymbol{\alpha} \otimes \mathbf{S} \cdot \boldsymbol{\alpha}.$$

The elastic energy can be decomposed in the following way:

$$(3.30) \qquad \Phi(\boldsymbol{\sigma}) = \Phi(\boldsymbol{\sigma}^\circ) + \Phi(\boldsymbol{\sigma}^*),$$

the following equality being true:

$$(3.31) \qquad \Phi(\boldsymbol{\sigma}^\circ) = \frac{1}{2}(\sigma^\circ)^2 \boldsymbol{\alpha} \cdot \mathbf{S} \cdot \boldsymbol{\alpha} = \frac{(\boldsymbol{\alpha} \cdot \mathbf{S} \cdot \boldsymbol{\alpha})^2}{2\boldsymbol{\alpha} \cdot \mathbf{S} \cdot \boldsymbol{\alpha}}.$$

Elastic energy of the hazardous part of stress is equal to

$$(3.32) \qquad \Phi(\boldsymbol{\sigma}^*) = \frac{1}{2}\boldsymbol{\sigma}^* \cdot \mathbf{S} \cdot \boldsymbol{\sigma}^* = \frac{1}{2}\boldsymbol{\sigma} \cdot \mathbf{S}^* \cdot \boldsymbol{\sigma},$$

where

$$(3.33) \quad \mathbf{S}^* \equiv (\mathbf{E}^*)^T \circ \mathbf{S} \circ \mathbf{E}^* = \mathbf{S} - (\mathbf{E}^\circ)^T \circ \mathbf{S} \circ \mathbf{E}^\circ = \mathbf{S} - \frac{1}{\boldsymbol{\alpha} \cdot \mathbf{S} \cdot \boldsymbol{\alpha}} \mathbf{S} \cdot \boldsymbol{\alpha} \otimes \mathbf{S} \cdot \boldsymbol{\alpha}.$$

Here $\mathbf{E}^*$ is a projector onto $\mathscr{E}^{\perp}$ parallel to $\mathscr{E}$, i.e.

$$(3.34) \qquad \mathbf{E}^* \cdot \boldsymbol{\sigma} \equiv \boldsymbol{\sigma}^* \qquad \text{for every} \qquad \boldsymbol{\sigma} \in \mathscr{S}.$$

Decomposition of the space (3.25) is associated with the corresponding decomposition of unit operator

$$(3.35) \qquad \mathbf{I} = \mathbf{E}^\circ + \mathbf{E}^*, \qquad \mathbf{E}^\circ \circ \mathbf{E}^* = \mathbf{E}^* \circ \mathbf{E}^\circ = \mathbf{0}.$$

For the bodies under consideration, the following **energy limit criterion** can be proposed

$$(3.36) \qquad \frac{1}{h}\Phi(\boldsymbol{\sigma}^*) \leq 1,$$

where h is the limit value of elastic energy under loading with the stress $\boldsymbol{\sigma}^* \in \mathscr{E}^{\perp}$. For the isotropic body with the spherical safe state, one has

$$(3.37) \qquad \begin{array}{cc} \boldsymbol{\alpha} = \mathbf{1}, & \mathbf{S} = \dfrac{1}{3K}\mathbf{I}_{\mathscr{P}} + \dfrac{1}{2G}\mathbf{I}_{\mathscr{D}}, \\[2mm] \mathbf{E}^\circ = \mathbf{I}_{\mathscr{P}}, & \mathbf{E}^* = \mathbf{I}_{\mathscr{D}}. \end{array}$$

Hence $\boldsymbol{\sigma}^* = \mathbf{s}$ and

$$(3.38) \qquad \Phi(\boldsymbol{\sigma}^*) = \Phi(\mathbf{s})$$

becomes the energy of shape change, and limit condition (3.36) turns out to be the Maxwell-Huber condition (1.7). Proposals [15] rely on the following two examples which excellently exhibit a difference between the isotropic and anisotropic bodies.

Example. *Let the hydrostatic stress states be safe*, i.e.

$$(3.39) \qquad \boldsymbol{\alpha} = \mathbf{1},$$

(see Fig. 1). Here

$$(3.40) \qquad \boldsymbol{\sigma}^\circ = \frac{\mathbf{1} \cdot \mathbf{S} \cdot \boldsymbol{\sigma}}{\mathbf{1} \cdot \mathbf{S} \cdot \mathbf{1}} \mathbf{1} = (9K\varepsilon)\mathbf{1},$$

$$(3.41) \qquad \boldsymbol{\sigma}^* = \boldsymbol{\sigma} - (9K\varepsilon)\mathbf{1}.$$

The space $\mathscr{E}^\perp$ is composed of the preserving volume stress states $\mathbf{1} \cdot \mathbf{S} \cdot \boldsymbol{\sigma}^* = 0$.
    Limit condition (3.36) takes the form

$$(3.42) \qquad \boldsymbol{\sigma} \cdot \mathbf{S} \cdot \boldsymbol{\sigma} - \frac{(\mathbf{1} \cdot \mathbf{S} \cdot \boldsymbol{\sigma})^2}{\mathbf{1} \cdot \mathbf{S} \cdot \mathbf{1}} \leq 2h.$$

This corresponds exactly to the first of the two possibilities proposed in [15].
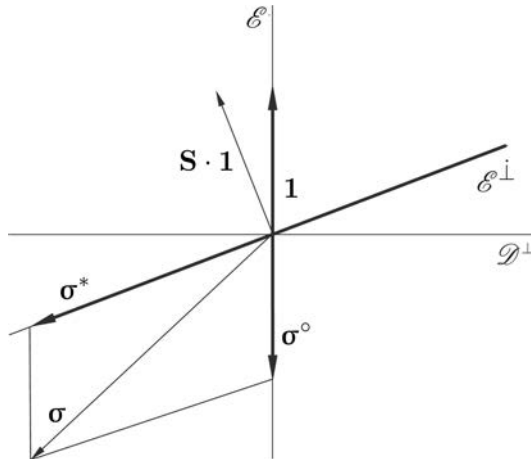
FIG. 3. $\mathscr{E}$ – space of spherical tensors, $\mathscr{E}^\perp$ – space of the preserving volume stresses, $\mathscr{D}^\perp$ – space of deviators.

Example. *Let every stress, which causes volume changes only, be safe.* Then

$$(3.43) \qquad \boldsymbol{\alpha} = \mathbf{C} \cdot \mathbf{1}$$

(see Fig. 4). Here

$$(3.44) \qquad \boldsymbol{\sigma}^\circ = \frac{3\sigma}{\mathbf{1} \cdot \mathbf{C} \cdot \mathbf{1}} \mathbf{C} \cdot \mathbf{1}, \qquad \sigma \equiv \frac{1}{3} \mathbf{1} \cdot \boldsymbol{\sigma},$$

$$(3.45) \qquad \boldsymbol{\sigma}^* = \boldsymbol{\sigma} - \frac{3\sigma}{\mathbf{1} \cdot \mathbf{C} \cdot \mathbf{1}} \mathbf{C} \cdot \mathbf{1}.$$
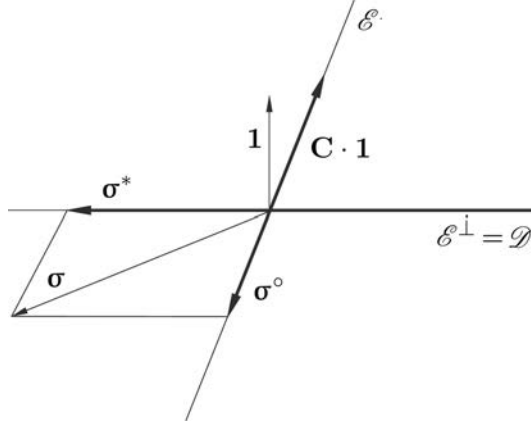
FIG. 4. $\mathscr{E}$ – space of stresses causing volume changes only, $\mathscr{D}$ – space of deviators.

Let us notice that $\boldsymbol{\sigma}^*$ is a deviator, $\mathbf{1} \cdot \boldsymbol{\sigma}^* = 0$ i.e. $\mathscr{E}^\perp = \mathscr{D}$. Deviator $\boldsymbol{\sigma}^*$ was introduced and interestingly implemented by V.A. LOMAKIN [20]. Limit condition in this case takes the form

$$(3.46) \qquad \boldsymbol{\sigma} \cdot \mathbf{S} \cdot \boldsymbol{\sigma} - \frac{9\sigma^2}{\mathbf{1} \cdot \mathbf{C} \cdot \mathbf{1}} \leq 2h.$$

This is the second possibility pointed out in [15].

For every *volumetrically-isotropic* body, particularly for an isotropic one, we have

$$(3.47) \qquad \mathbf{S} \cdot \mathbf{1} = \frac{1}{3K} \mathbf{1}, \qquad \mathbf{C} \cdot \mathbf{1} = (3K)\mathbf{1}$$

and both conditions (3.42) and (3.46) coincide.

Unfortunately, criterion (3.36) is of a very particular nature. Limit properties are described here, with the exception of one constant h fixing the scale of stress, with the elastic tensor $\mathbf{S}^*$ alone. Such close bonds between the limit and the elastic properties seem to be very particular and can not take place in a general case of anisotropic body.

We should notice also that it is not difficult to generalize the obtained relations on the case when the space of the safe states is not one-dimensional.

4. Principal decomposition of the elastic energy

We need now a short, but crucial for the further considerations, excursion to some section of the algebra of Euclidean tensors, which is not known well enough and not sufficiently exploited in mechanics.

The set $\mathscr{S}$ can be considered as a linear 6-dimensional space with the scalar product

$$(4.1) \qquad (\boldsymbol{\alpha}, \boldsymbol{\beta}) \rightarrow \boldsymbol{\alpha} \cdot \boldsymbol{\beta}.$$

Let us take two arbitrary bases in $\mathscr{S}$, i.e. two linearly independent sets of symmetric second-rank tensors

$$(4.2) \qquad \begin{aligned} \boldsymbol{\nu}_G, \qquad & G = \mathrm{I}, \mathrm{II}, \ldots, \mathrm{VI}, \\ \boldsymbol{\mu}_l, \qquad & l = \mathrm{I}, \mathrm{II}, \ldots, \mathrm{VI}. \end{aligned}$$

According to the very definition of the tensor product of the linear spaces, a system of 36 *fourth* rank tensors

$$(4.3) \qquad \boldsymbol{\nu}_G \otimes \boldsymbol{\mu}_l \qquad G, l = \mathrm{I}, \mathrm{II}, \ldots, \mathrm{VI}$$

constitute a basis in $\mathscr{T} \equiv \mathscr{S} \overline{\otimes} \mathscr{S}$. Hence any tensor $\mathbf{L} \in \mathscr{T}$ can be uniquely denoted as

$$(4.4) \qquad \mathbf{L} = \sum_{G,l=\mathrm{I}}^{\mathrm{VI}} L_{Gl} \boldsymbol{\nu}_G \otimes \boldsymbol{\mu}_l.$$

Moreover, it is convenient to regard any tensor $\mathbf{L} \in \mathscr{T}$ as *a linear operator* from $\mathscr{S}$ into $\mathscr{S}$, acting according to the rule

$$(4.5) \qquad \boldsymbol{\alpha} \rightarrow \mathbf{L} \cdot \boldsymbol{\alpha},$$

where $(\boldsymbol{\omega} \otimes \boldsymbol{\tau}) \cdot \boldsymbol{\alpha} \equiv (\boldsymbol{\tau} \cdot \boldsymbol{\alpha}) \boldsymbol{\omega}$.

Let us introduce, for the basis $\boldsymbol{\mu}_l$, its standard reciprocal basis $\boldsymbol{\mu}^l$. It is defined as the unique solution of the system of equations

$$(4.6) \qquad \boldsymbol{\mu}_l \cdot \boldsymbol{\mu}^k = \delta_l^k \equiv \begin{cases} 1 & l = k, \\ 0 & l \neq k. \end{cases}$$

Now $\mathbf{L} \cdot \boldsymbol{\mu}^l = L_{\mathrm{I}\,l} \boldsymbol{\nu}_\mathrm{I} + L_{\mathrm{II}\,l} \boldsymbol{\nu}_\mathrm{II} + \ldots$ and, hence, Eq. (4.4) can be expressed as the *fundamental identity*: for any $\mathbf{L} \in \mathscr{T}$ and any basis $\boldsymbol{\mu}_K$ in $\mathscr{S}$,

$$(4.7) \quad \mathbf{L} = \mathbf{L} \cdot \boldsymbol{\mu}^\mathrm{I} \otimes \boldsymbol{\mu}_\mathrm{I} + \ldots + \mathbf{L} \cdot \boldsymbol{\mu}^\mathrm{VI} \otimes \boldsymbol{\mu}_\mathrm{VI} = \mathbf{L} \cdot \boldsymbol{\mu}_\mathrm{I} \otimes \boldsymbol{\mu}^\mathrm{I} + \ldots + \mathbf{L} \cdot \boldsymbol{\mu}_\mathrm{VI} \otimes \boldsymbol{\mu}^\mathrm{VI}.$$

Let us come back to the idea of energy decomposition, which by no means can be reduced to the examples quoted in Sec. 3.

Let us analyze a symmetric bilinear form $\boldsymbol{\alpha} \cdot \mathbf{S} \cdot \boldsymbol{\beta}$. It is a polar form of the positive defined quadratic form $\boldsymbol{\alpha} \cdot \mathbf{S} \cdot \boldsymbol{\alpha}$ on $\mathscr{S}$. Therefore an operation

$$(4.8) \qquad (\boldsymbol{\alpha} \cdot \boldsymbol{\beta}) \to \boldsymbol{\alpha} \times \boldsymbol{\beta} \equiv \boldsymbol{\alpha} \cdot \mathbf{S} \cdot \boldsymbol{\beta}$$

defines another correct scalar product of symmetric tensors of rank two. We shall call it **energy-scalar product**, contrary to the **standard scalar product** $\boldsymbol{\alpha} \cdot \boldsymbol{\beta}$. Energy product $\boldsymbol{\alpha} \times \boldsymbol{\beta}$ is tailored to the particular elastic body under consideration, it is defined by its compliance tensor $\mathbf{S}$. The condition of the energy-separation $\boldsymbol{\alpha} \cdot \mathbf{S} \cdot \boldsymbol{\beta} = 0$ achieves the geometric meaning of orthogonality in energy sense

$$\boldsymbol{\alpha} \overset{.}{\perp} \boldsymbol{\beta}, \quad \text{i.e.} \quad \boldsymbol{\alpha} \times \boldsymbol{\beta} = 0.$$

Elastic energy of the stress is equal to one half of the square of the energy-norm of $\boldsymbol{\sigma}$:

$$(4.9) \qquad \Phi(\boldsymbol{\sigma}) = \frac{1}{2} \boldsymbol{\sigma} \times \boldsymbol{\sigma}.$$

Definition. Every decomposition

$$(4.10) \qquad \mathscr{S} = \mathscr{E}_1 \oplus, \ldots, \oplus \mathscr{E}_{\varkappa}, \qquad \varkappa \le 6,$$

for which any two components of the direct sum are energy-orthogonal (separated)

$$(4.11) \qquad \mathscr{E}_{\alpha} \overset{.}{\perp} \mathscr{E}_{\beta} \quad \text{for} \quad \alpha \ne \beta,$$

we shall call an **energy-orthogonal decomposition** of the stress space for a given elastic body.

Distributing any stress tensor over subspaces (4.10)

$$(4.12) \qquad \boldsymbol{\sigma} = \boldsymbol{\sigma}_1 + \ldots + \boldsymbol{\sigma}_{\varkappa}, \qquad \boldsymbol{\sigma}_{\alpha} \in \mathscr{E}_{\alpha},$$

we have

$$(4.13) \qquad \boldsymbol{\sigma}_{\alpha} \times \boldsymbol{\sigma}_{\beta} = 0 \quad \text{for} \quad \alpha \ne \beta$$

and, hence, as it should be,

$$(4.14) \qquad \Phi(\boldsymbol{\sigma}_1 + \ldots + \boldsymbol{\sigma}_{\varkappa}) = \Phi(\boldsymbol{\sigma}_1) + \ldots + \Phi(\boldsymbol{\sigma}_{\varkappa}).$$

Of course, there exist many energy-orthogonal decompositions at will.

Let us introduce a projector $\mathbf{E}_\alpha$ on the subspace $\mathscr{E}_\alpha$ parallel to $\mathscr{E}^\perp = \mathscr{E}_1 \oplus \ldots \oplus \mathscr{E}_{\alpha-1} \oplus \mathscr{E}_{\alpha+1} \oplus \ldots \oplus \mathscr{E}_\varkappa$

$$(4.15) \qquad \mathbf{E}_\alpha \cdot \boldsymbol{\omega} = \begin{cases} \boldsymbol{\omega} & \text{if} \quad \boldsymbol{\omega} = \mathscr{E}_\alpha, \\ \mathbf{0} & \text{if} \quad \boldsymbol{\omega} \perp \mathscr{E}_\alpha. \end{cases}$$

Decomposition of the unity operator

$$(4.16) \qquad \mathbf{I} = \mathbf{E}_1 + \ldots + \mathbf{E}_\varkappa,$$

corresponds to the decomposition (4.10), here

$$(4.17) \qquad \mathbf{E}_\alpha \circ \mathbf{E}_\alpha = \mathbf{E}_\alpha, \qquad \mathbf{E}_\alpha \circ \mathbf{E}_\beta = \mathbf{0} \quad \text{for} \quad \alpha \neq \beta.$$

It is not difficult to express projectors $\mathbf{E}_\alpha$ explicitly. Let us take any energy-orthonormal basis

$$(4.18) \qquad \begin{array}{c} \mathbf{\partial}_\mathrm{I}, \ldots, \mathbf{\partial}_\mathrm{VI}, \\ \mathbf{\partial}_K \times \mathbf{\partial}_L = \delta_{KL} \equiv \begin{cases} 1 & K = L, \\ 0 & K \neq L, \end{cases} \end{array}$$

chosen in such a way, that the first s_1 elements. $\mathbf{\partial}_1, \ldots, \mathbf{\partial}_{s_1}$ belong to $\mathscr{E}_1, s_1 = \dim \mathscr{E}_1$, the next s_2 belong to $\mathscr{E}_2$, etc. The reciprocal basis will assume the following form:

$$(4.19) \qquad \mathbf{\partial}^\mathrm{I} \equiv \mathbf{S} \cdot \mathbf{\partial}_\mathrm{I}, \ldots, \mathbf{\partial}^\mathrm{VI} \equiv \mathbf{S} \cdot \mathbf{\partial}_\mathrm{VI}.$$

Indeed

$$(4.20) \qquad \mathbf{\partial}_K \cdot \mathbf{\partial}^L = \mathbf{\partial}_K \times \mathbf{\partial}_L = \delta_{KL}.$$

If one considers $\mathbf{\partial}_K$ as a stress, then $\mathbf{\partial}^K$ will be the strain caused by this stress. Using identity (4.7), one obtains promptly

$$(4.21) \qquad \mathbf{E}_1 = \mathbf{\partial}_\mathrm{I} \otimes \mathbf{\partial}^\mathrm{I} + \ldots + \mathbf{\partial}_{s_1} \otimes \mathbf{\partial}^{s_1}.$$

Let us notice the following relations yielding from (4.7):

$$(4.22) \qquad \mathbf{S} = \mathbf{\partial}^\mathrm{I} \otimes \mathbf{\partial}^\mathrm{I} + \ldots + \mathbf{\partial}^\mathrm{VI} \otimes \mathbf{\partial}^\mathrm{VI},$$

$$(4.23) \qquad \mathbf{C} = \mathbf{\partial}_\mathrm{I} \otimes \mathbf{\partial}_\mathrm{I} + \ldots + \mathbf{\partial}_\mathrm{VI} \otimes \mathbf{\partial}_\mathrm{VI}.$$

The most remarkable among the energy-decompositions is the decomposition pointed out and applied in papers [19, 21–24]. It is given by the following theorem being some implementation of the general spectral theorem (see c.f. [25, 26]).

Theorem: *For every elastic body, defined with its compliance tensor* $\mathbf{S}$, *there exists exactly one energy-orthogonal and orthogonal decomposition*

$$(4.24) \qquad \mathscr{S} = \mathscr{P}_1 \oplus \ldots \oplus \mathscr{P}_\varrho, \qquad \varrho \le 6,$$

$$(4.25) \qquad \mathscr{P}_\alpha \overset{\cdot}{\perp} \mathscr{P}_\beta, \qquad \mathscr{P}_\alpha \perp \mathscr{P}_\beta, \qquad \text{for} \quad \alpha \ne \beta$$

and exactly one set of pair-wise unequal constants

$$(4.26) \qquad \lambda_1, \ldots, \lambda_\varrho, \qquad \lambda_\alpha \ne \lambda_\beta \qquad \text{for} \quad \alpha \ne \beta$$

such, that

$$(4.27) \qquad \mathbf{S} = \frac{1}{\lambda_1}\mathbf{P}_1 + \ldots + \frac{1}{\lambda_\varrho}\mathbf{P}_\varrho,$$

where $\mathbf{P}_\alpha$ *is an orthogonal projector on* $\mathscr{P}_\alpha$, $\alpha = 1, \ldots, \varrho$.

Proof. Since $\mathbf{S}$ is a symmetric operator acting in the space $\mathscr{S}$ with the scalar product (4.1), the equation

$$(4.28) \qquad \mathbf{S} \cdot \boldsymbol{\omega} = \frac{1}{\lambda}\boldsymbol{\omega}$$

has an orthonormal set of solutions

$$(4.29) \qquad \begin{gathered} \boldsymbol{\omega}_{\mathrm{I}}, \ldots, \boldsymbol{\omega}_{\mathrm{VI}}, \\ \boldsymbol{\omega}_K \cdot \boldsymbol{\omega}_L = \delta_{KL}, \end{gathered}$$

each $\boldsymbol{\omega}_K$ being related to the proper value λ_K^{-1}. This orthonormal basis is accompanied by the energy-orthonormal one

$$(4.30) \qquad \mathfrak{z}_1 = \lambda_{\mathrm{I}}^{1/2}\boldsymbol{\omega}_{\mathrm{I}}, \ldots, \quad \mathfrak{z}_{\mathrm{VI}} = \lambda_{\mathrm{VI}}^{1/2}\boldsymbol{\omega}_{\mathrm{VI}}$$

and

$$(4.31) \qquad \mathfrak{z}^{\mathrm{I}} = \frac{1}{\lambda_{\mathrm{I}}^{1/2}}\boldsymbol{\omega}_{\mathrm{I}}, \ldots, \quad \mathfrak{z}^{\mathrm{VI}} = \frac{1}{\lambda_{\mathrm{VI}}^{1/2}}\boldsymbol{\omega}_{\mathrm{VI}}.$$

From (4.22) it follows that

$$(4.32) \qquad \mathbf{S} = \frac{1}{\lambda_{\mathrm{I}}}\boldsymbol{\omega}_{\mathrm{I}} \otimes \boldsymbol{\omega}_{\mathrm{I}} + \ldots + \frac{1}{\lambda_{\mathrm{VI}}}\boldsymbol{\omega}_{\mathrm{VI}} \otimes \boldsymbol{\omega}_{\mathrm{VI}}.$$

Let $\boldsymbol{\omega}_K$ are labeled in such a way, that

$$\lambda_{\mathrm{I}} = \lambda_{\mathrm{II}} = \ldots = \lambda_{s_1} = \lambda_1, \quad \lambda_{s_1+1} = \ldots = \lambda_{s_1+s_2} = \lambda_2$$

etc., then

$$(4.33) \qquad \boldsymbol{\omega}_{\mathrm{I}} \otimes \boldsymbol{\omega}_{\mathrm{I}} + \ldots + \boldsymbol{\omega}_{s_1} \otimes \boldsymbol{\omega}_{s_1} = \mathbf{P}_1,$$

are orthogonal projectors on some subspaces

$$\mathscr{P}_1, \ldots; \dim \mathscr{P}_1 = s_1, \ldots$$

Expression (4.32) takes the form of (4.27). It is evident that the decomposition (4.24) is unique, orthogonal and energy-orthogonal. From (4.23) it follows, that

$$(4.34) \qquad \mathbf{C} = \lambda_1 \mathbf{P}_1 + \ldots + \lambda_\varrho \mathbf{P}_\varrho.$$

Solutions $\boldsymbol{\omega}$ of the Eq. (4.28) we designed in [19] as **proper elastic states** of the elastic body under consideration, while parameters λ were called **true** (**proper**) **stiffness moduli**[3]. The proper elastic states have been found for all symmetries of crystals and the anisotropic engineering materials.

Spaces $\mathscr{P}_\alpha$ consist of the proper elastic states and to each of these spaces is prescribed its own true stiffness modulus λ_α. We shall call (4.24) **the proper energy-decomposition**, for the body under consideration.

Let us represent arbitrary stress $\boldsymbol{\sigma}$ according to the proper decomposition:

$$(4.35) \qquad \boldsymbol{\sigma} = \boldsymbol{\sigma}_1 + \ldots + \boldsymbol{\sigma}_\varrho, \qquad \boldsymbol{\sigma}_\alpha \equiv \mathbf{P}_\alpha \cdot \boldsymbol{\sigma} \in \mathscr{P}_\alpha;$$

$$(4.36) \qquad \boldsymbol{\sigma}_\alpha \cdot \boldsymbol{\sigma}_\beta = 0, \qquad \text{for} \quad \alpha \neq \beta.$$

We introduce also values of projections

$$(4.37) \qquad \sigma_\alpha \equiv (\boldsymbol{\sigma}_\alpha \cdot \boldsymbol{\sigma}_\alpha)^{1/2} = (\boldsymbol{\sigma} \cdot \mathbf{P}_\alpha \cdot \boldsymbol{\sigma})^{1/2}.$$

The elastic energy corresponding to the α-th part of the stress is equal to

$$(4.38) \qquad \Phi(\boldsymbol{\sigma}_\alpha) \equiv \frac{1}{2} \boldsymbol{\sigma}_\alpha \cdot \mathbf{S} \cdot \boldsymbol{\sigma} = \frac{\sigma_\alpha^2}{2\lambda_\alpha}, \qquad \alpha = 1, \ldots, \varrho$$

and, therefore, **the proper decomposition of energy** (corresponding to the proper space decomposition) takes a very simple form

$$(4.39) \qquad \Phi(\boldsymbol{\sigma}) = \frac{\sigma_1^2}{2\lambda_1} + \ldots + \frac{\sigma_\varrho^2}{2\lambda_\varrho}.$$

---

[3] The Author referred to them also as to **Kelvin moduli**, cf. J. RYCHLEWSKI, On Hooke's Law, *Journal of Applied Mathematics and Mechanics*, 48(3), 303–314, 1984 (translator's remark).

Basing on this foundation, one can propose the following *particular quadratic energy-criterion of the limit state*:

$$(4.40) \qquad \frac{\sigma_1^2}{k_1^2} + \ldots + \frac{\sigma_\varrho^2}{k_\varrho^2} \leq 1,$$

where $h_\alpha \equiv k_\alpha^2/2\lambda_\alpha$ is the limit value of energy of the load $\boldsymbol{\sigma}_\alpha \in \mathscr{P}_\alpha$. If $k_\alpha = \infty$, then the space $\mathscr{P}_\alpha$ is composed of the safe states.

For the materials being isotropic with respect to elastic properties, the proper elastic states are following: any hydrostatic stress $\boldsymbol{\sigma}_1 = \sigma\mathbf{1}$ with the stiffness modulus $\lambda_1 = 3K$ and any deviator $\boldsymbol{\sigma}_2 = \mathbf{s}$, with the stiffness modulus $\lambda_2 = 2G$. Principal decomposition is given by the expression (3.18) and structural one (4.27) – by the relation (3.15). Hence, the limit criterion (4.40) can be expressed as

$$(4.41) \qquad \frac{\sigma^2}{\sigma_0^2} + \frac{\mathbf{s} \cdot \mathbf{s}}{2k^2} \leq 1.$$

If any hydrostatic state is safe, then $\sigma_0 = \infty$ and we obtain the Maxwell–Huber criterion (1.1).

Criterion (4.40) assumes some *weak coupling between elastic and limit properties*. In many cases such a coupling probably takes place, e.g. due to the symmetry of the structure of the body under consideration. However it can not be truthfully in a general case. The simplest counterexample supplies a body which is isotropic as regards its elastic properties, being anisotropic regarding limit properties. We shall fully clarify the nature of the specific connection between the elastic and the limit properties in the Sec. 6.

Comment. On the ground of (4.39) one can propose, of course, a more general energy-criterion

$$(4.42) \qquad F(\sigma_1, \ldots, \sigma_\varrho) \leq 1;$$

it would, however still, enclose an assumption about the mentioned interconnection between the elastic and the limit properties.

5. ENERGY RELATED MEANING OF THE QUADRATIC LIMIT CRITERIA

Noticeable, ahead evident, generalization of the condition (1.1) was proposed in the classic work of R. VON MISES [27]. He has chosen the yield condition in the form

$$(5.1) \qquad \mathbf{s} \cdot \mathbf{H} \cdot \mathbf{s} \leq 1,$$

where $\mathbf{H} \in \mathscr{T}$. For $\mathbf{H} = (1/2k^2)\mathbf{I}_{\mathscr{D}}$ one obtains (1.1). It was repeated by R. Hill for orthotropic bodies in [28].

We shall discuss the most general **quadratic condition of limit state**

$$(5.2) \qquad\qquad \boldsymbol{\sigma} \cdot \mathbf{H} \cdot \boldsymbol{\sigma} \leq 1.$$

We shall call tensor $\mathbf{H}$ the **limit state tensor** and the quadratic form $\boldsymbol{\sigma} \cdot \mathbf{H} \cdot \boldsymbol{\sigma}$ will be called a **quadratic measure of stress intensity**. Without loss of generality one can assume, that $\mathbf{H}$ is a symmetric tensor of $\mathscr{T}$. Besides this, the measure of intensity of an arbitrary load $\boldsymbol{\sigma}$ should be non-negative. Thus, the following conditions are imposed on $\mathbf{H}$:

$$(5.3) \qquad \mathbf{H} = \mathbf{H}^T, \qquad \boldsymbol{\alpha} \cdot \mathbf{H} \cdot \boldsymbol{\alpha} \geq 0 \qquad \text{for any} \quad \boldsymbol{\alpha} \in \mathscr{S}.$$

As always, with the quadratic form $\boldsymbol{\alpha} \cdot \mathbf{H} \cdot \boldsymbol{\alpha}$ are associated: its polar – bilinear symmetric form $\boldsymbol{\alpha} \cdot \mathbf{H} \cdot \boldsymbol{\beta}$ and the symmetric linear operator $\mathbf{H}\cdot$, $\boldsymbol{\alpha} \rightarrow \mathbf{H} \cdot \boldsymbol{\alpha}$. We shall make use of this operator without delay.

A stress state $\boldsymbol{\sigma}$ we shall call the **safe state** for the elastic body, whose limit properties are given by the limit state tensor $\mathbf{H}$ if $\boldsymbol{\sigma} \cdot \mathbf{H} \cdot \boldsymbol{\sigma} = 0$. Let us recall the simple theorem of linear algebra.

Theorem. *The set of the safe stress states constitutes a kernel of the operator* $\mathbf{H}\cdot$, *i.e. it is composed of the stresses* $\boldsymbol{\sigma}$, *fulfilling the condition*

$$(5.4) \qquad\qquad \mathbf{H} \cdot \boldsymbol{\sigma} = \mathbf{0}.$$

Proof. Let us examine measure of stress intensity on a unit sphere $\boldsymbol{\sigma} \cdot \boldsymbol{\sigma} = 1$. Due to non-negativeness, its null value is minimal. Therefore: if $\boldsymbol{\sigma} \cdot \mathbf{H} \cdot \boldsymbol{\sigma} = 0$, then the derivative of the Lagrange function $\boldsymbol{\sigma} \cdot \mathbf{H} \cdot \boldsymbol{\sigma} - \mu(\boldsymbol{\sigma} \cdot \boldsymbol{\sigma} - 1)$ must vanish, this yields $\mathbf{H} \cdot \boldsymbol{\sigma} = \mu\boldsymbol{\sigma}$, at the same time $\mu = \boldsymbol{\sigma} \cdot \mathbf{H} \cdot \boldsymbol{\sigma}/\boldsymbol{\sigma} \cdot \boldsymbol{\sigma} = 0$.

Von Mises criterion (5.1) is in fact a criterion (5.2) for which it was assumed that an arbitrary hydrostatic stress is safe. Then $\mathbf{1} \cdot \mathbf{H} \cdot \mathbf{1} = 0$, i.e.

$$(5.5) \qquad\qquad \mathbf{H} \cdot \mathbf{1} = \mathbf{1} \cdot \mathbf{H} = \mathbf{0}$$

and, therefore

$$\boldsymbol{\sigma} \cdot \mathbf{H} \cdot \boldsymbol{\sigma} = \mathbf{s} \cdot \mathbf{H} \cdot \mathbf{s}.$$

This assumption does not seem to us to be naturally innate in general case. There are no a priori reasons for considering a spherical tensor as something exceptional for anisotropic media. *The habit to separate the spherical part of stress* $\sigma\mathbf{1}$ *and to consider the pressure* $-\sigma$ *as some universal thermodynamic parameter, has come into mechanics of the solid deformable body from the mechanics and thermodynamics of liquids and gases and has rooted on fertile soil*

of isotropic bodies. This habit should be revised, in our opinion. In particular, for the anisotropic body, say a composite, quite different stress states related to its structure (reinforcement, etc.) can emerge as the safe ones.

Concerning the limit state tensor $\mathbf{H}$ we shall not assume anything more than (5.3).

R. von Mises have not ascribed any specific interpretation to his condition. In particular, any connection of his measure of stress intensity $\mathbf{s} \cdot \mathbf{H} \cdot \mathbf{s}$ with elastic energy was not discernible. We shall prove that an *arbitrary quadratic measure of stress intensity $\boldsymbol{\sigma} \cdot \mathbf{H} \cdot \boldsymbol{\sigma}$ possesses uniquely defined, in terms of energy, interpretation.* This is contained in the following theorem, which is an implementation of the idea o simultaneous reduction of two quadratic forms (here $\boldsymbol{\sigma} \cdot \mathbf{H} \cdot \boldsymbol{\sigma}$ and $\boldsymbol{\sigma} \cdot \mathbf{S} \cdot \boldsymbol{\sigma}$) into a sum of squares (cf. [29]).

Theorem. *For every elastic body defined by its compliance tensor $\mathbf{S}$ and limit state tensor $\mathbf{H}$, there exist: exactly one energy-orthogonal decomposition*:

$$(5.6) \qquad \mathscr{S} = \mathscr{H}_1 \oplus \ldots \oplus \mathscr{H}_\chi, \qquad \chi \le 6,$$

$$(5.7) \qquad \mathscr{H}_\alpha \perp \mathscr{H}_\beta \qquad \text{for} \qquad \alpha \ne \beta$$

and exactly one set of pair-wise unequal constants

$$(5.8) \qquad h_1, \ldots, h_\chi, \qquad h_\alpha \ne h_\beta, \qquad \text{for} \qquad \alpha \ne \beta,$$

such that, for an arbitrary stress

$$(5.9) \qquad \boldsymbol{\sigma} = \boldsymbol{\sigma}_1 + \ldots + \boldsymbol{\sigma}_\chi, \qquad \boldsymbol{\sigma}_\alpha \in \mathscr{H}_\alpha,$$

the measure of stress intensity is equal to

$$(5.10) \qquad \boldsymbol{\sigma} \cdot \mathbf{H} \cdot \boldsymbol{\sigma} = \frac{1}{h_1}\Phi(\boldsymbol{\sigma}_1) + \ldots + \frac{1}{h_\chi}\Phi(\boldsymbol{\sigma}_\chi),$$

where

$$(5.11) \qquad \Phi(\boldsymbol{\sigma}_1) + \ldots + \Phi(\boldsymbol{\sigma}_\chi) = \Phi(\boldsymbol{\sigma}).$$

Proof. We shall present a constructive one. We shall entirely use the energy-scalar product (4.8) instead of the standard one (4.1). Let us introduce linear operations

$$(5.12) \qquad \mathbf{L} \times \boldsymbol{\alpha} \equiv \mathbf{L} \cdot (\mathbf{S} \cdot \boldsymbol{\alpha}) = (\mathbf{L} \circ \mathbf{S}) \cdot \boldsymbol{\alpha},$$

$$(5.13) \qquad \boldsymbol{\alpha} \times \mathbf{L} \equiv (\mathbf{S} \cdot \boldsymbol{\alpha}) \cdot \mathbf{L} = (\boldsymbol{\alpha} \cdot \mathbf{S}) \cdot \mathbf{L} = \boldsymbol{\alpha} \cdot (\mathbf{S} \circ \mathbf{L}),$$

$$(5.14) \qquad \mathbf{L} \,\square\, \mathbf{N} \equiv \mathbf{L} \circ \mathbf{S} \circ \mathbf{N}.$$

We shall identify tensors $\mathbf{L} \in \mathscr{T}$ with linear operators acting from $\mathscr{S}$ into $\mathscr{S}$, according to the rule

$$(5.15) \qquad\qquad \boldsymbol{\alpha} \to \mathbf{L} \times \boldsymbol{\alpha}$$

instead of (4.5). Unit operator $\boldsymbol{\alpha} \to \boldsymbol{\alpha}$ under this convention is realized not by the tensor $\mathbf{I}$, but by the stiffness tensor $\mathbf{C}$. Indeed,

$$(5.16) \qquad\qquad \mathbf{C} \times \boldsymbol{\alpha} = (\mathbf{C} \circ \mathbf{S}) \cdot \boldsymbol{\alpha} = \mathbf{I} \cdot \boldsymbol{\alpha} = \boldsymbol{\alpha}.$$

Let us write the stress intensity measure in the following form:

$$(5.17) \qquad\qquad \boldsymbol{\alpha} \times (\mathbf{C} \circ \mathbf{H} \circ \mathbf{C}) \times \boldsymbol{\alpha} = \boldsymbol{\alpha} \cdot \mathbf{H} \cdot \boldsymbol{\alpha}.$$

The operation completed by the tensor $\mathbf{C} \circ \mathbf{H} \circ \mathbf{C}$ is symmetric with respect to the energy-scalar product, i.e.

$$(5.18) \qquad\qquad \boldsymbol{\alpha} \times (\mathbf{C} \circ \mathbf{H} \circ \mathbf{C}) \times \boldsymbol{\beta} = \boldsymbol{\beta} \times (\mathbf{C} \circ \mathbf{H} \circ \mathbf{C}) \times \boldsymbol{\alpha}$$

for every $\boldsymbol{\alpha}, \boldsymbol{\beta} \in \mathscr{S}$. Let us analyze proper elements $\boldsymbol{\chi}$ and proper values $(2h)^{-1}$ of this operator

$$(5.19) \qquad\qquad (\mathbf{C} \circ \mathbf{H} \circ \mathbf{C}) \times \boldsymbol{\chi} = \frac{1}{2h}\boldsymbol{\chi}.$$

In view of the symmetry (5.18) one can evidently find an energy-orthonormal set of solutions

$$(5.20) \qquad\qquad \boldsymbol{\chi}_{\mathrm{I}}, \ldots, \boldsymbol{\chi}_{\mathrm{VI}}, \qquad \boldsymbol{\chi}_K \times \boldsymbol{\chi}_L = \delta_{KL},$$

where $\boldsymbol{\chi}_L$ corresponds to the proper value $(2h_L)^{-1}$. The set of $\boldsymbol{\chi}_K \otimes \boldsymbol{\chi}_L$ constitutes a basis in $\mathscr{T}$ (see (4.4)) i.e. for any $\mathbf{L} \in \mathscr{T}$

$$(5.21) \qquad\qquad \mathbf{L} = \sum_{K,L=\mathrm{I}}^{\mathrm{VI}} L_{KL}\boldsymbol{\chi}_K \otimes \boldsymbol{\chi}_L;$$

here

$$(5.22) \qquad\qquad L_{KL} \equiv \boldsymbol{\chi}_K \times \mathbf{L} \times \boldsymbol{\chi}_L.$$

In particular, taking into account (5.19) and (5.20), for $\mathbf{L} = \mathbf{C} \circ \mathbf{H} \circ \mathbf{C}$ one has:

$$(5.23) \qquad \mathbf{C} \circ \mathbf{H} \circ \mathbf{C} = \frac{1}{2h_{\mathrm{I}}}\boldsymbol{\chi}_{\mathrm{I}} \otimes \boldsymbol{\chi}_{\mathrm{I}} + \ldots + \frac{1}{2h_{\mathrm{VI}}}\boldsymbol{\chi}_{\mathrm{VI}} \otimes \boldsymbol{\chi}_{\mathrm{VI}}.$$

Let χ_K be labeled in such a way that $h_I = \ldots = h_{G_1} = h_1$, $h_{G_1+1} = \ldots = h_{G_2+2} = h_2$ etc. Let us consider

$$(5.24) \qquad \mathbf{H}_1 \equiv \chi_1 \otimes \chi_1 + \ldots + \chi_{G_1} \otimes \chi_{G_1}$$
....

and denote

$$(5.25) \qquad \mathscr{H}_1 \equiv \operatorname{Im} H_1 \ldots, \qquad \dim \mathscr{H}_1 = G_1, \ldots$$

It is evident that

$$(5.26) \qquad \mathbf{H}_\alpha \times \chi = \begin{cases} \chi & \text{for} \quad \chi \in H_\alpha, \\ \mathbf{0} & \text{for} \quad \chi \in H_\beta, \quad \beta \neq \alpha \end{cases}$$

and $\mathscr{H}_\alpha \dot{\perp} \mathscr{H}_\beta$ for $\alpha \neq \beta$. In other words, $\mathbf{H}_\alpha$ are energy-orthoprojectors and constitute energy-orthogonal decomposition of the unity operator

$$(5.27) \qquad \mathbf{C} = \mathbf{H}_1 + \ldots + \mathbf{H}_\chi,$$

$$(5.28) \qquad \mathbf{H}_\alpha \,\square\, \mathbf{H}_\alpha = \mathbf{H}_\alpha, \qquad \mathbf{H}_\alpha \,\square\, \mathbf{H}_\beta = \mathbf{0} \qquad \text{for} \quad \alpha \neq \beta.$$

It corresponds to space decomposition (5.6), (5.7).

Collecting together in (5.23) the terms with the same h_L, one obtains

$$(5.29) \qquad \mathbf{C} \circ \mathbf{H} \circ \mathbf{C} = \frac{1}{2h_1}\mathbf{H}_1 + \ldots + \frac{1}{2h_\chi}\mathbf{H}_\chi.$$

Taking (5.9) we get (5.11). Now

$$(5.30) \qquad \boldsymbol{\sigma} \cdot \mathbf{H} \cdot \boldsymbol{\sigma} = \frac{1}{2h_1}\boldsymbol{\sigma} \times \mathbf{H}_1 \times \boldsymbol{\sigma} + \ldots + \frac{1}{2h_\chi}\boldsymbol{\sigma} \times \mathbf{H}_\chi \times \boldsymbol{\sigma}$$

and, since

$$(5.31) \qquad \boldsymbol{\sigma} \times \mathbf{H}_\alpha \times \boldsymbol{\sigma} = \boldsymbol{\sigma}_\alpha \times \boldsymbol{\sigma}_\alpha = 2\Phi(\boldsymbol{\sigma}_\alpha)$$

we obtain (5.10).

Everything here is constructed effectively, together with the definitions of h_K and χ_K using the Eq. (5.19), which can be rewritten as

$$(5.32) \qquad (2h\mathbf{H} - \mathbf{S}) \cdot \chi = \mathbf{0}.$$

The expression for the limit state tensor can be expressed as follows:

$$(5.33) \qquad \mathbf{H} = \frac{1}{2h_I}\mathbf{S} \cdot \chi_I \otimes \mathbf{S} \cdot \chi_I + \ldots + \frac{1}{2h_{VI}}\mathbf{S} \cdot \chi_{VI} \otimes \mathbf{S} \cdot \chi_{VI},$$

or

$$(5.34) \qquad \mathbf{H} = \frac{1}{2h_{\mathrm{I}}}\mathbf{S}_1 + \ldots + \frac{1}{2h_{\chi}}\mathbf{S}_{\chi},$$

where

$$(5.35) \qquad \mathbf{S}_\alpha \equiv \mathbf{S} \circ \mathbf{H}_\alpha \circ \mathbf{S}, \qquad \alpha = 1, \ldots, \chi,$$

$$(5.36) \qquad \mathbf{S} = \mathbf{S}_1 + \ldots + \mathbf{S}_{\chi}.$$

Thus, **any arbitrary quadratic criterion of limit state can be expressed in the form of energy-inequality**

$$(5.37) \qquad \frac{1}{h_1}\Phi(\boldsymbol{\sigma}_1) + \ldots + \frac{1}{h_{\chi}}\Phi(\boldsymbol{\sigma}_{\chi}) \le 1.$$

Parameters

$$(5.38) \qquad h_\alpha \equiv \frac{\boldsymbol{\chi} \cdot \mathbf{S} \cdot \boldsymbol{\chi}}{2\boldsymbol{\chi} \cdot \mathbf{H} \cdot \boldsymbol{\chi}} = \text{const} \qquad \text{for any} \quad \boldsymbol{\chi} \in \mathscr{H}_\alpha$$

are the limit values of elastic energy for the loads $\boldsymbol{\sigma}_\alpha \in \mathbf{H}_\alpha$.

If $h_\alpha = \infty$, then the loads $\boldsymbol{\sigma}_\alpha \in \mathscr{H}_\alpha$ are safe. Criteria (3.42) and (3.46) represent particular cases of (5.37) for

$$(5.39) \qquad \chi = 2, \qquad h_1 = \infty, \qquad \dim \mathscr{H}_1 = 1.$$

Let us notice that expression (5.33) presents the most general form of limit state tensor in such a sense, that $\mathbf{H}$ is uniquely determined by some energy-orthogonal basis $\boldsymbol{\chi}_K$ and a set of h_K

$$(5.40) \qquad (h_1, \ldots, h_{\mathrm{VI}}; \ \boldsymbol{\chi}_{\mathrm{I}}, \ldots, \boldsymbol{\chi}_{\mathrm{VI}}) \to \mathbf{H}.$$

6. On possible forms of coupling between the elastic and the limit properties

Theorem (5.10) does not assume any connection between the directional distribution of the elastic properties described by the compliance tensor $\mathbf{S}$ and the limit properties described by the limit state tensor $\mathbf{H}$. Though, some coupling may appear due to the structure of the body. Our theorem points out a form through which this coupling may possibly reveal itself.

The principal decomposition of elastic energy (4.24) differs from the decomposition with regard to limit properties (5.6) by its orthogonality. Let us make clear when (5.6) is also orthogonal. We shall start from the following lemma:

Lemma. *Energy-orthogonal decomposition*

$$(6.1) \qquad \mathscr{S} = \mathscr{E}_1 \oplus \ldots \oplus \mathscr{E}_{\varkappa}, \qquad \varkappa \le 6$$

is orthogonal if and only if it is stable (invariant) with respect to the compliance tensor **S**.

Proof. Sufficiency. Let the energy-orthogonal decomposition be stable with respect to **S**, i.e. $\mathbf{S} \cdot \boldsymbol{\omega} \in \mathscr{E}_\alpha$ for each $\boldsymbol{\omega} \in \mathscr{E}_\alpha$ and for all $\alpha = 1, \ldots, \varkappa$. Then in any $\mathscr{E}_\alpha$ one can find a basis $\boldsymbol{\omega}_1, \ldots, \boldsymbol{\omega}_q$, $q = \dim \mathscr{E}_\alpha$ consisting of the proper elements of **S**,

$$(6.2) \qquad \mathbf{S} \cdot \boldsymbol{\omega}_K = \mu_K \boldsymbol{\omega}_K, \qquad K = 1, \ldots, q,$$

where $\mu_K > 0$, i.e. the form $\boldsymbol{\alpha} \cdot \mathbf{S} \cdot \boldsymbol{\alpha}$, is positive definite. Let us take any $\boldsymbol{\alpha} \in \mathscr{E}_\alpha$ and any $\boldsymbol{\beta} \in \mathscr{E}_\beta$, $\boldsymbol{\beta} \neq \boldsymbol{\alpha}$. Since $\mathscr{E}_\alpha \dot{\perp} \mathscr{E}_\beta$, then

$$(6.3) \quad \boldsymbol{\alpha} \cdot \boldsymbol{\beta} = (\alpha_1 \boldsymbol{\omega}_1 + \ldots + \alpha_q \boldsymbol{\omega}_q) \cdot \boldsymbol{\beta} = \left(\frac{\alpha_1}{\mu_1} \mathbf{S} \cdot \boldsymbol{\omega}_1 + \ldots + \frac{\alpha_q}{\mu_q} \mathbf{S} \cdot \boldsymbol{\omega}_q \right) \cdot \boldsymbol{\beta}$$

$$= \frac{\alpha_1}{\mu_1} \boldsymbol{\omega}_q \times \boldsymbol{\beta} + \ldots + \frac{\alpha_q}{\mu_q} \boldsymbol{\omega}_q \times \boldsymbol{\beta} = 0,$$

i.e. $\mathscr{E}_\alpha \perp \mathscr{E}_\beta$.

Necessity. Let any two terms of energy-orthogonal decomposition be orthogonal, i.e.

$$(6.4) \qquad \mathscr{E}_\alpha \dot{\perp} \mathscr{E}_\beta \qquad \text{and} \qquad \mathscr{E}_\alpha \perp \mathscr{E}_\beta \qquad \text{for all} \qquad \alpha \neq \beta.$$

Let us take arbitrary $\mathscr{E}_\alpha$. In virtue of (6.4), an orthogonal complement $\mathscr{E}_\alpha^\perp$ coincides with the energy-orthogonal one $\mathscr{E}_\alpha^{\dot{\perp}}$. Therefore for any $\boldsymbol{\alpha} \in \mathscr{E}_\alpha$, taking any $\boldsymbol{\tau} \in \mathscr{E}_\alpha^\perp$ we have $\boldsymbol{\alpha} \times \boldsymbol{\tau} = \boldsymbol{\alpha} \cdot \mathbf{S} \cdot \boldsymbol{\tau} = 0$, i.e. $\mathbf{S} \cdot \boldsymbol{\alpha} \in \mathscr{E}_\alpha^{\perp\perp} = \mathscr{E}_\alpha$. Therefore any $\mathscr{E}_\alpha$ is invariant with respect to **S**.

Definition. We shall tell that $\mathbf{A}, \mathbf{B} \in \mathscr{T}$ are **coaxial** if there exists an orthonormal basis

$$(6.5) \qquad \boldsymbol{\omega}_1, \ldots, \boldsymbol{\omega}_{\mathrm{VI}}, \qquad \boldsymbol{\omega}_K \cdot \boldsymbol{\omega}_L = \delta_{KL},$$

composed of the proper elements of both tensors, i.e. such, that for some sets $\alpha_{\mathrm{I}}, \ldots, \alpha_{\mathrm{VI}}$ and $\beta_{\mathrm{I}}, \ldots, \beta_{\mathrm{VI}}$:

$$(6.6) \qquad \begin{aligned} \mathbf{A} &= \alpha_{\mathrm{I}} \boldsymbol{\omega}_{\mathrm{I}} \otimes \boldsymbol{\omega}_{\mathrm{I}} + \ldots + \alpha_{\mathrm{VI}} \boldsymbol{\omega}_{\mathrm{VI}} \otimes \boldsymbol{\omega}_{\mathrm{VI}}, \\ \mathbf{B} &= \beta_{\mathrm{I}} \boldsymbol{\omega}_{\mathrm{I}} \otimes \boldsymbol{\omega}_{\mathrm{I}} + \ldots + \beta_{\mathrm{VI}} \boldsymbol{\omega}_{\mathrm{VI}} \otimes \boldsymbol{\omega}_{\mathrm{VI}}. \end{aligned}$$

Let us notice that the numbers of equal values in the array $\alpha_{\mathrm{I}}, \ldots, \alpha_{\mathrm{VI}}$ can be entirely different from those of $\beta_{\mathrm{I}}, \ldots, \beta_{\mathrm{VI}}$. Hence, decompositions of $\mathscr{S}$ into direct sums of the proper subspaces of **A** and **B** can be quite different.

Theorem. *Energy-orthogonal decomposition of the stress space with regard to the limit properties of the body (5.6) is orthogonal if and only if the limit state tensor* $\mathbf{H}$ *and the compliance tensor* $\mathbf{S}$ *are coaxial.*

Proof. Necessity. Let a decomposition (5.6) be orthogonal. This means, according to the lemma, that it is stable with respect to the $\mathbf{S}$. Therefore, there exists such an orthonormal basis $\boldsymbol{\omega}_{\mathrm{I}}, \ldots, \boldsymbol{\omega}_{\mathrm{VI}}$, composed of the proper elements of $\mathbf{S}$, that any $\boldsymbol{\omega}_K$ belongs to one of $\mathscr{E}_\alpha$. For any $\boldsymbol{\chi} \in \mathscr{E}_\alpha$, however, Eq. (5.32) is satisfied with some value of h. Thus, for any $\boldsymbol{\omega}_K$, $\mathbf{H} \cdot \boldsymbol{\omega}_K = \nu_K \boldsymbol{\omega}_K$ for a certain ν_K, i.e. basis $\boldsymbol{\omega}_K$ is composed of proper elements of the tensor $\mathbf{H}$. Sufficiency. Assume that $\mathbf{H}$ and $\mathbf{S}$ are coaxial, $\boldsymbol{\omega}_K$ being an orthonormal basis composed of proper elements of $\mathbf{S}$ and $\mathbf{H}$. Then $\boldsymbol{\chi}_K = \boldsymbol{\omega}_K$ satisfy Eq. (5.32). Carried out according to relations (5.24), decomposition (5.6) is, therefore, orthogonal.

Coaxiality of the tensors $\mathbf{S}$, $\mathbf{H}$

$$(6.7) \qquad \mathbf{S} = \frac{1}{\lambda_{\mathrm{I}}} \boldsymbol{\omega}_{\mathrm{I}} \otimes \boldsymbol{\omega}_{\mathrm{I}} + \ldots + \frac{1}{\lambda_{\mathrm{VI}}} \boldsymbol{\omega}_{\mathrm{VI}} \otimes \boldsymbol{\omega}_{\mathrm{VI}},$$

$$(6.8) \qquad \mathbf{H} = \frac{1}{2h_{\mathrm{I}}} \boldsymbol{\omega}_{\mathrm{I}} \otimes \boldsymbol{\omega}_{\mathrm{I}} + \ldots + \frac{1}{2h_{\mathrm{VI}}} \boldsymbol{\omega}_{\mathrm{VI}} \otimes \boldsymbol{\omega}_{\mathrm{VI}},$$

reflects some coupling between the elastic and the limit properties. It does not seem to be very rigid.

We shall present the following interpretation of the coaxiality (6.7), (6.8). For any quadratic form $\boldsymbol{\sigma} \cdot \mathbf{A} \cdot \boldsymbol{\sigma}$, the states of local extremality, defined by the condition

$$(6.9) \qquad \boldsymbol{\sigma} \cdot \mathbf{A} \cdot \boldsymbol{\sigma} = \mathrm{ext} \quad \mathrm{at} \quad \boldsymbol{\omega} \cdot \boldsymbol{\omega} = 1, \quad \mathrm{under\ condition} \quad \boldsymbol{\sigma} \cdot \mathbf{A} \cdot \boldsymbol{\sigma} = 1$$

are the proper elements, i.e.

$$(6.10) \qquad\qquad \mathbf{A} \cdot \boldsymbol{\sigma} = \alpha \boldsymbol{\sigma}.$$

Indeed, (6.9) is equivalent to

$$(6.11) \qquad \partial_\sigma F = 0 \quad \mathrm{for} \quad F \equiv \boldsymbol{\sigma} \cdot \mathbf{A} \cdot \boldsymbol{\sigma} - \alpha(\boldsymbol{\sigma} \cdot \boldsymbol{\sigma} - 1)$$

which yields Eq. (6.10).

Proper elastic states $\mathbf{S} \cdot \boldsymbol{\omega} = (1/\lambda)\boldsymbol{\omega}$ are, therefore, **the states of extremal energy** and the proper states of $\mathbf{H}$, $\mathbf{H} \cdot \boldsymbol{\omega} = \chi \boldsymbol{\omega}$ are **the states of extremal limit stress measure**.

Coaxiality of $\mathbf{S}$ and $\mathbf{H}$, therefore, means that there exists an orthonormal set of states $\boldsymbol{\omega}_K$ being simultaneously the states of extremal energy and the states of maximal limit stress intensity, see Fig. 5.
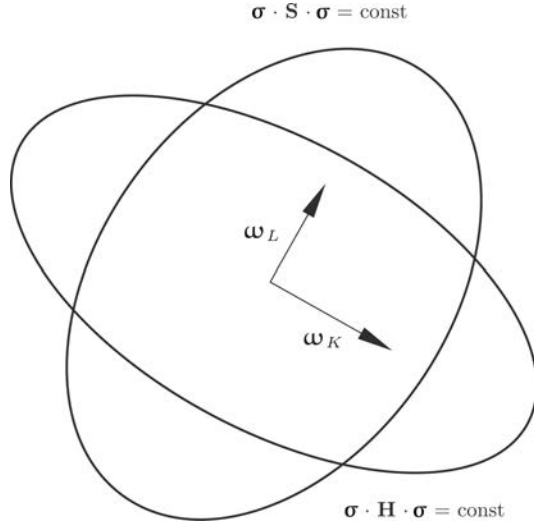
$$\boldsymbol{\sigma} \cdot \mathbf{S} \cdot \boldsymbol{\sigma} = \text{const}$$

$$\boldsymbol{\sigma} \cdot \mathbf{H} \cdot \boldsymbol{\sigma} = \text{const}$$

FIG. 5. Coaxiality of the compliance tensor $\mathbf{S}$ and the limit state tensor $\mathbf{H}$, the cross-section of the surface of equal energy and the surface of the equal limit stress intensity with the plane $(\boldsymbol{\omega}_L, \boldsymbol{\omega}_K)$ in the stress space.

Let us consider a more restrictive modification of a coupling between the elastic and the limit properties, where *any state of extremal energy is simultaneously the state of extremal limit stress measure*. This is a particular case of coaxiality when

$$(6.12) \qquad\qquad \lambda_K = \lambda_L \Rightarrow h_K = h_L.$$

Taking the structural decomposition of the compliance tensor

$$(6.13) \qquad\qquad \mathbf{S} = \frac{1}{\lambda_1}\mathbf{P}_1 + \ldots + \frac{1}{\lambda_\varrho}\mathbf{P}_\varrho,$$

where $\lambda_\alpha \neq \lambda_\beta$ for $\alpha \neq \beta$, one has

$$(6.14) \qquad\qquad \mathbf{H} = \frac{1}{2h_1}\mathbf{P}_1 + \ldots + \frac{1}{2h_\varrho}\mathbf{P}_\varrho,$$

values of h_α being not necessarily different. Just in this case, a quadratic limit criterion takes the form (4.40).

7. Expression of any limit criterion in the E. Beltrami form

As we have already mentioned, E. BELTRAMI in his unjustly forgotten paper [10] posed a limit criterion

$$(7.1) \qquad\qquad \Phi(\boldsymbol{\sigma}) \leq h = \text{ const.}$$

This proposal meets at once the following objection: for overwhelming majority of circumstances, hydrostatic stress can be considered as safe. We shall, however, *not throw the baby out with the bathwater*. A rational root of E. Beltrami proposal consists in the fact that for the failure of element, one always needs to spend some work, which, in the elastic element, should be equal to the elastic energy stored until that instant. Shortcoming of the direct realization of this concept in the form of (7.1) lies only in the assumption that this work does not depend on the kind of stress state.

Let us introduce and denote as $h(\boldsymbol{\omega})$, $\boldsymbol{\omega} \cdot \boldsymbol{\omega} = 1$, *the limit value of elastic energy which the element is capable to accumulate under the load* $\boldsymbol{\sigma} = c\boldsymbol{\omega}$, $c > 0$. For the usual elastic body (hyperelastic), $h(\boldsymbol{\omega})$ is equal to the work, which is necessary for failure of the element under such stress. W shall modify the proposal of E. Beltrami as follows:

$$(7.2) \qquad \Phi(\boldsymbol{\sigma}) \leq h\left(\frac{\boldsymbol{\sigma}}{(\boldsymbol{\sigma} \cdot \boldsymbol{\sigma})^{1/2}}\right).$$

But such a form can assume any limit criterion for which the region of the safe states in $\mathscr{S}$ has a stellar shape and includes unstressed natural state; an overdone example is shown in Fig. 6. Indeed, any such a region is described by inequality

$$(7.3) \qquad \boldsymbol{\sigma} \cdot \boldsymbol{\sigma} \leq k^2\left(\frac{\boldsymbol{\sigma}}{(\boldsymbol{\sigma} \cdot \boldsymbol{\sigma})^{1/2}}\right),$$
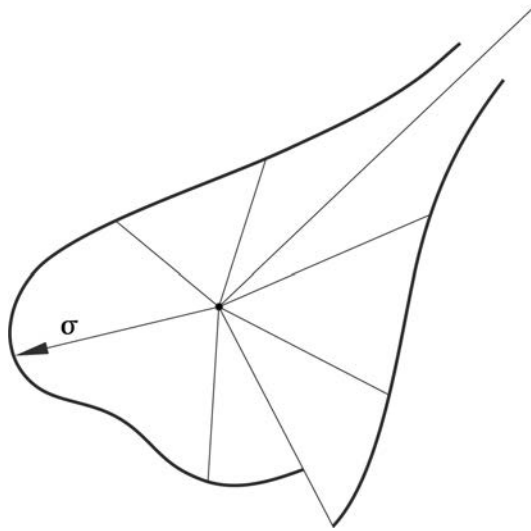

Fɪɢ. 6. An exotic example of a star-shape region of safe states, containing unstressed natural state.

where k is the limit function defined on the unit sphere in $\mathscr{S}$. Since for linearly elastic body one has

$$(7.4) \qquad \Phi(\boldsymbol{\sigma}) = (\boldsymbol{\sigma} \cdot \boldsymbol{\sigma})\Phi\left(\frac{\boldsymbol{\sigma}}{(\boldsymbol{\sigma} \cdot \boldsymbol{\sigma})^{1/2}}\right),$$

then (7.3) is equivalent to (7.2) with

$$(7.5) \qquad h(\boldsymbol{\omega}) = \Phi(\boldsymbol{\omega})k^2(\boldsymbol{\omega}).$$

Since the expressed assumption regarding the shape of the region of safe states is fulfilled for all thinkable cases (materials, processes, kinds of limit properties), representation (7.2) is not confined to any kind of particular form of limit criterion.

For the quadratic criteria of limit states (5.2) considered above

$$(7.6) \qquad k^2(\boldsymbol{\omega}) = (\boldsymbol{\omega} \cdot \mathbf{H} \cdot \boldsymbol{\omega})^{-1} = [h_1\Phi(\boldsymbol{\omega}_1) + \ldots + h_\chi\Phi(\boldsymbol{\omega}_\chi)]^{-1}.$$

where

$$(7.7) \qquad \begin{aligned} \boldsymbol{\omega} &= \boldsymbol{\omega}_1 + \ldots + \boldsymbol{\omega}_\chi, \qquad \boldsymbol{\omega}_\alpha \in \mathscr{H}_\alpha, \\ \boldsymbol{\omega}_1 \cdot \boldsymbol{\omega}_1 &= \ldots = \boldsymbol{\omega}_\chi \cdot \boldsymbol{\omega}_\chi = 1. \end{aligned}$$

The Maxwell–Huber criterion represented in E. Beltrami form looks as follows:

$$(7.8) \qquad \Phi(\boldsymbol{\sigma}) \le h + l\frac{\sigma^2}{\mathbf{s} \cdot \mathbf{s}},$$

where

$$(7.9) \qquad h \equiv \frac{k^2}{2G}, \qquad l \equiv \frac{k^2}{K}.$$

Quadratic criteria are discussed from somewhat different viewpoint in [30].

8. Conclusions

Simple, but unexpected theorem (5.10) exhausts in a formal sense the problem of energy-criteria of the limit state which, for isotropic bodies, was posed by Maxwell, Beltrami and Huber.

This problem was transferred in the Polish school of mechanics along the relay of generations, from M.T. Huber to W. Burzyński and W. Olszak, from W. Olszak to W. Urbanowski, an from them to J. Ostrowska. I am obliged to her for discussions which helped me to clarify this history of the subject. I am also grateful to N.N. Malinin for his kind discussions, during which he proved to be an expert on Polish works.

APPENDIX 1

List of equivalences, making possible to transform readily any expression of this paper to the standard Cartesian index notation with the usual summation rules:

$$\boldsymbol{\sigma}, \boldsymbol{\varepsilon}, \boldsymbol{\alpha} \quad \leftrightarrow \quad \sigma_{ij}, \varepsilon_{ij}, \alpha_{ij},$$

$$\mathbf{1}, \mathbf{s} \quad \leftrightarrow \quad \delta_{ij}, s_{ij},$$

$$\mathbf{C}, \mathbf{S}, \mathbf{H} \quad \leftrightarrow \quad C_{ijkl}, S_{ijkl}, H_{ijkl},$$

$$\boldsymbol{\alpha} \cdot \boldsymbol{\beta} \quad \leftrightarrow \quad \alpha_{ij}\beta_{ij},$$

$$\boldsymbol{\alpha} \times \boldsymbol{\beta} \quad \leftrightarrow \quad S_{ijkl}\alpha_{ij}\beta_{kl},$$

$$\boldsymbol{\alpha} \otimes \boldsymbol{\beta} \quad \leftrightarrow \quad \alpha_{ij}\beta_{kl},$$

$$\mathbf{L} \cdot \boldsymbol{\alpha} \quad \leftrightarrow \quad L_{ijkl}\alpha_{kl},$$

$$\boldsymbol{\alpha} \cdot \mathbf{L} \cdot \boldsymbol{\beta} \quad \leftrightarrow \quad L_{ijkl}\alpha_{ij}\beta_{kl},$$

$$\mathbf{A}^T = \mathbf{A} \quad \leftrightarrow \quad A_{ijkl} = A_{klij},$$

$$\mathbf{A} \circ \mathbf{B} \quad \leftrightarrow \quad A_{ijpq}B_{pqkl},$$

$$\partial_\varepsilon \varPhi \quad \leftrightarrow \quad \frac{\partial \varPhi}{\partial \varepsilon_{kl}}$$

$$\mathbf{I}_{ijkl} = \frac{1}{2}(\delta_{ik}\delta_{jl} + \delta_{il}\delta_{kj}).$$

In the whole paper, $\mathscr{S}$ is the space of the symmetric Euclidean tensors of second rank and $\mathscr{T}$ denotes its tensorial product

$$\mathscr{T} \equiv \mathscr{S} \otimes \mathscr{S}.$$

Tensors of stiffness $\mathbf{C}$, compliance $\mathbf{S}$ and limit state $\mathbf{H}$ obey conditions of internal symmetry

$$A_{ijkl} = A_{jikl} = A_{klij}.$$

In the whole paper, besides the present Appendix, the summation over repeated indices is not applied.

APPENDIX 2

We quote this fragment of the letter of J.C. Maxwell, [from Origins of Clerk Maxwell's Electric Ideas. . . [5], pp. 31–33], which had a chance to become a foundation of contemporary mathematical theory of plasticity.

129 Union Street
Aberdeen
18 Dec. 1856

Dear Thomson

. . . .

Here is my present notion about plasticity of homogeneous amorphous solids.

Let $\alpha\beta\gamma$ be the 3 principal strains at any point PQR the principal stresses connected with $\alpha\beta\gamma$ by symmetrical linear equations the same for all axes. Then the whole work done by PQR in developing may be written

$$U = A(\alpha^2 + \beta^2 + \gamma^2) + B(\beta\gamma + \gamma\alpha + \alpha\beta)$$

where A and B are coeffts, the nature of which is foreign to our inquiry. Now we may put

$$U = U_1 + U_2,$$

where U_1 is due to a symmetrical compression ($\alpha_1 = \beta_1 = \gamma_1$) and U_2 to distortion without compression ($\alpha_2 + \beta_2 + \gamma_2 = 0$)

$$\alpha = \alpha_1 + \alpha_2, \qquad \beta = \beta_1 + \beta_2, \qquad \gamma = \gamma_1 + \gamma_2.$$

It follows that $\qquad U_1 = 1/3(A + B)(\alpha + \beta + \gamma)^2$

$$U_2 = \frac{2A - B}{3}\left(\alpha^2 + \beta^2 + \gamma^2 - (\beta\gamma + \gamma\alpha + \alpha\beta)\right).$$

Now my *opinion* is that these two parts may be considered as independent U_1 being the work done in condensation and U_2 that done in distortion. Now I would use the old word "Resilience" to denote the work necessary to be done on a body to overcome its elastic forces.

The cubical resilience R is a measure of the work necessary to be expended in compression in order to increase the density permanently. This *must* increase rapidly as the body is condensed, whether it be wood or lead or iron.

The resilience of rigidity R_2 (which is the converse of plasticity) is the work required to be expended in pure distortion in order to produce a permanent change of form in the element. I have strong reasons for believing that when

$$\alpha^2 + \beta^2 + \gamma^2 - \beta\gamma - \gamma\alpha - \alpha\beta$$

reaches a certain limit $= R_2$ then the element will begin to give way. If the body be tough the disfigurement will go on till this function U_2 (which truly represents the work which the element *would* do in recovering its form) has diminished to R by an alteration of the *permanent dimensions.*

Now let $a\,b\,c$ be the *very small* permanent alterations due to the fact that $U_2 > R_2$ for an instant. Whenever $U_2 = R_2$ the element has as much work done to it as it can bear. Any more work done to the element will be consumed in parmanent alterations.

Therefore if $U_2 = R_2$, and in the next instant, U be increased, dU must be lost in some way.

My rough notion on this subject is that

$$a = \frac{dU}{U}\alpha, \qquad b = \frac{dU}{U}\beta, \qquad c = \frac{dU}{U}\gamma$$

the new values of α β γ will be

$$\alpha' = \alpha - a, \qquad \beta' = \beta - b, \qquad \gamma' = \gamma - c.$$

This is the first time that I have put pen to paper on this subject. I have never seen any investigation of the question, „Given the mechanical strain in 3 directions on an element, when will it give way?" I think this notion will bear working out into a mathemat. theory of plasticity when I have time; to be compared with experiment when I know the right experiments to make.

Condition of not yielding

$$\alpha^2 + \beta^2 + \gamma^2 - \beta\gamma - \gamma\alpha - \alpha\beta < R_2.$$

Yours

J.C. Maxwell

References

1. M. T. Huber, *Specific work of strain as a measure of material effort* [in Polish], Czasopismo Techniczne, XXII, Lwow, 1904, also English translation: Arch. Mech., **56**, 173–190, 2004.

2. R. Mises, *Mechanik der festen Körper im plastisch-deformablen Zustand*, Nachr. von der Königlichen Geselschaft der Wissenschaften zu Götingen, Math. Phys., 1, Kl. 4, 582–592, 1913.

3. H. Hencky, *Zur Theorie plastischer Deformationen und der hierdurch im Material hervorgerufenen Nachspannungen*, ZAMM, **4**, 323–334, 1924.

4. H. Mierzejewski, *Foundations of Mechanics of Plastic Solids* [in Polish], Warszawa, 1927.

5. J. C. Maxwell, Proc. Cambridge Phil. Soc., 32, 1936 (cf. also: Origins of Clerk Maxwell's electric ideas as described in familiar letters to William Thompson, ed. by Sir J. Larmor, Cambridge at Univ. Press, 1937).

6. G. Green, *On the laws of the reflection and refraction of light at the common surface of two non-crystallized media*, Trans. Of the Cambridge Phil. Soc., VII, 1–24, 1839 (cf. also: Math. Papers of the late George Green, 1971).

7. G. G. Stokes, *On the theories of the internal friction of fluids in motion of elastic solids*, Trans. of the Cambridge Phil. Soc., VIII, 287–319, 1849 (cf. also Math. Papers, I, 75–129).

8. H. Helmhotz, *Dynamic continuerlich verbreiteten Massen*, Leipzig, 1902.

9. A. Föppl, L. Föppl, *Drang und Zwang*, I, München u. Berlin, 1920.

10. E. BELTRAMI, *Sulla conditioni di resistenza dei corpi elastici*, Rend. Ist. Lomb., II, 18, 1885.

11. B. P. HIGH, *Strain-energy function and elastic limit*, Rpt. Brit.Association for the Advancement of Sciences, 486, 1919, Engineering, CIX, 158–160, 1920.

12. W. BURZYŃSKI, *Studium nad hipotezami wytężenia*, Lwów, 1928 (cf. also: Dzieła Wybrane, t. I, PWN, Warszawa, 1982, 67–258; and English translation: *Selected passages from Włodzimierz Burzyński's doctoral dissertation Study on Material Effort Hypotheses*, Engineering Transactions, **57**, 3–4, 185–215, 2009.

13. M. M. FILONENKO–BORODICH, *Mechanical theories of strength* [in Russian], Izd. MGU, Moskva 1961.

14. V. V. NOVOZHILOV, *About physical meaning of stress invariants* [in Russian], Prikl. Mat. Mekh, **15**, 2, 1951.

15. W. OLSZAK, W. URBANOWSKI, *The plastic potential and the generalized distortion energy*, Arch. Mech. Stos., **8**, 4, 1956.

16. W. OLSZAK, J. OSTROWSKA–MACIEJEWSKA, *The plastic potential in the theory of anisotropic elastic-plastic bodies*, Engineering Fracture Mechanics, **21**, 625–632, 1985.

17. A. L. CAUCHY, *Sur les équations différentielles d'equilibre ou de mouvement pour un systéme de points matériels sollicités par des forces d'attraction ou de répulsion mutuelle*, Exercises de mathématiques, **4**, 129–139, 1829.

18. I. TODHUNTER, K. PEARSON, *A history of the theory of elasticity and of the strength of materials*, I, Univ. Press, Cambridge, 1886.

19. J. RYCHLEWSKI, ≪*CEIIINOSSSTTUV*≫ *Mathematical structure of elastic bodies* [in Russian], Institut Problem Mekhaniki AN SSSR, preprint 217, 1983.

20. V. A. LOMAKHIN, *About the non-linear theory of elasticity and plasticity of anisotropic continua* [in Russian], Izv. AN SSSR, OTN Mekh. i Mashinnostr., **4**, 60–64, 1960.

21. J. RYCHLEWSKI, *Dinh laut Hooke hong cach mo ta moi*, Bao cao tai HOI THAO QUOC TE CO HOC, Hanoi, **4**, 252–256, 1983.

22. J. RYCHLEWSKI, *On thermoelastic constants*, Arch. Mech., **36**, 1, 77–95, 1984.

23. J. RYCHLEWSKI, *About Hooke's law* [in Russian], Prikl. Mat. Mekh., 48, 420–435, 1984; also in English: J. Applied Mathematics and Mechanics, **48**, 303–314, 1984.

24. J. RYCHLEWSKI, *About the non-coaxiality of elastic deformations and stresses* [in Russian], Izv. RAN MTT, 101–104, 1984.

25. A. I. MALCEV, *Foundations of Linear Algebra* [in Russian], Gostexizdat, Moskva, 1956.

26. I. M. GLAZMAN, YU. I. LYUBICH, *Finite dimensional linear analysis* [in Russian], Nayka, Moskva, 1969.

27. R. MISES, *Mechanik der plastischen Formänderung von Kristallen*, ZAMM, **8**, 161–185, 1928.

28. R. HILL, *The Mathematical Theory of Plasticity*, Clarendon Press, Oxford, 1950.

29. I. M. GELFAND, *Lectures on Linear Algebra* [in Russian], Nayka, Moskva, 1971.

30. J. RYCHLEWSKI, *About quadratic limit criteria of stressed state* [in Russian] – manuscript.

Summary

The well-known yield condition for isotropic materials, known as the M.T. Hu-ber (and R. von Mises, H. Hencky) yield condition, has oryginally been proposed by J.C. Maxwell (see Appendix 2) in 1856. Maxwell and Huber atttributed the following physical sense to the criterion: the material stays elastic as long as the distortion energy does not reach the critical value. The attempt made by W. Olszak and W. Urbanowski, who tried to generalize the criterion to anisotropic bodies, is not convincing owing to the fact that, in the case of anisotropic media, decomposition of the total elastic energy into the parts connected with the change of volume and the change of shape is impossible.

The notion of "energy-ortogonal" states of stress is introduced in the paper. One state of stress is energy-orthogonal to another state of stress if the first one does not perform any work along the deformations produced by the other. The following theorem is proved: each limit criterion may be represented as a certain condition imposed upon a linear combination of elastic energies corresponding to a uniquely determined (for the given material) pari-wise energy-orthogonal, additive components of the total state of stress. Hence, each quadratic criterion has a definite energy interpretation. Moreover, it is shown that each limit criterion may be written in the form of an ineguality bounding the accumulated elastic energy. Considered are also the problems of possible forms of coupling of elastic properties of materials with the corresponding limit criteria.

INSTYTUT PODSTAWOWYCH   Obtained March 25, 1984
PROBLEMÓW TECHNIKI PAN
UL. ŚWIĘTOKRZYSKA 21
00-049 WARSZAWA

Translator's note

My schoolmate, friend and tutor in science Jan Rychlewski is bodily still among us, but his heavy disease makes not possible the author's supervision over the translation. Keeping this in mind, the translator tried to avoid, if possible, any more important departures from a literal translation. This was a difficult task. Russian phrasing of Jan was extremely rich and colorful. He is in fact a Russian native speaker. Being an ethnic Pole born in USSR, he was in early childhood separated from his family in result of sad events of year 1938. During his mature years spent in Poland, he maintained close connection with the Russian culture and language. Neither English nor Russian is a translator's native tongue (however he believes that his Russian is much better than English). Thus, despite the translator's efforts to make his best, sometimes the results may occur to be odd. The whole responsibility for his lack of competence in the linguistic matter, the translator takes on his shoulders. The only justification can be his will to pay his debt of gratitude to the diseased friend.

Andrzej Blinowski

————————

Contents of issue 1   vol. LIX